ACCEPTED VERSION

C. Burton, P. Visintin, M. Griffith, J. Vaculik
Laboratory investigation of pull-out capacity of chemical anchors in individual new and vintage masonry units under quasi-static, cyclic and impact load
Structures, 2021; 34:901-930

© 2021 Institution of Structural Engineers. Published by Elsevier Ltd. All rights reserved.

This manuscript version is made available under the CC-BY-NC-ND 4.0 license
http://creativecommons.org/licenses/by-nc-nd/4.0/

Final publication at: http://dx.doi.org/10.1016/j.istruc.2021.08.016

PERMISSIONS

https://www.elsevier.com/about/policies/sharing

Accepted Manuscript

Authors can share their accepted manuscript:

24 Month Embargo

After the embargo period

- via non-commercial hosting platforms such as their institutional repository
- via commercial sites with which Elsevier has an agreement

In all cases accepted manuscripts should:

- link to the formal publication via its DOI
- bear a CC-BY-NC-ND license – this is easy to do
- if aggregated with other manuscripts, for example in a repository or other site, be shared in alignment with our hosting policy
- not be added to or enhanced in any way to appear more like, or to substitute for, the published journal article

1 March 2024

http://hdl.handle.net/2440/133799

LABORATORY INVESTIGATION OF PULL-OUT CAPACITY OF CHEMICAL ANCHORS IN INDIVIDUAL NEW AND VINTAGE MASONRY UNITS UNDER QUASI-STATIC, CYCLIC AND IMPACT LOAD

Burton, C., Visintin, P., Griffith, M., Vaculik, J.

Published version at: Burton, C., Visintin, P., Griffith, M. and Vaculik, J., Laboratory Investigation of Pull-out Capacity of Chemical Anchors in Individual New and Vintage Masonry Units Under Quasi-static, Cyclic and Impact Load.

Abstract

Failure of unreinforced masonry following the 2011 Christchurch earthquake demonstrated that many masonry strengthening solutions were inadequate for the peak ground accelerations that were experienced, and also that many of the failures were associated with underperformance of masonry anchors. Recent in-situ pull-out tests of anchors in vintage masonry structures has identified that in these tests, the failure is predominantly via splitting of the masonry units. This finding is in contrast to current design approaches that only consider failure via the formation of a cone or wedge, or masonry unit extraction. To further examine the potential for unit splitting prior to the failure modes identified in current design approaches, a laboratory campaign investigating masonry unit properties and anchor pull-out capacities, covering quasi-static, cyclic and impact loading of anchors and also incorporating the influence of quality of installation is reported here. The results of this campaign confirm that the unit splitting is an important failure mode, which may explain the observed anchorage underperformance. It is further observed that whilst cyclic and impact loading, as well as poor quality of installation have a detrimental effect on anchor performance, performance nonetheless exceeds published characteristic strengths. Additionally, as part of the laboratory campaign, a simple method for supporting masonry test units has been developed which has demonstrated good replication of the in-situ test results.

1. Introduction

Historically, masonry structures (e.g. places of worship) were reliant on their physical bulk for stability, to minimise tensile stresses, and to provide shear capacity through friction to resist lateral loads from wind and earthquake (Page 2002). More recently, there exists a large stock of lighter (vintage) masonry construction that was built prior to the development of an understanding of seismic loading and the requirement for seismic design. This form of construction is typified by laterally unrestrained parapet walls and gable ends, often looming over footpaths and narrow streets, and because these vintage structures lack the physical bulk of historic structures they are especially susceptible to seismic loading. Following research into seismic loading and development of earthquake design codes, strengthening of unreinforced masonry (URM) structures and components has been undertaken in many jurisdictions. For example, in New Zealand, construction of URM structures was notionally banned following the publication of NZSS no. 95, *New Zealand Standard Model Building By-Law* which was a direct consequence of the Hawkes Bay earthquake in 1931 (Megget 2006). By 2004, (through the New Zealand Building Act 2004) earthquake-prone buildings, including all buildings other than small residential structures were required to be strengthened. Despite this intervention, the principal cause of fatalities in the 2010 Christchurch earthquake (which had peak ground accelerations (PGAs) at or just above design code values), and the 2011 event (where the PGAs were well above design code values), were associated with URM buildings.

In these events, 39 out of 42 fatalities occurred "outside" the structure as a result of falling masonry (Moon et al. 2014). Significantly, a number of the failures that resulted in fatalities involved URM structures that had previously been strengthened, thereby demonstrating that the strengthening solutions previously adopted were ineffective. In a later analysis of these structural failures, Dizhur et al. (2016) reported that in many instances it was the connection of the masonry to the retrofitted strengthening that failed, and that the anchors had underperformed.

Anchoring or fastening of elements to masonry is not new; Vitruvius in the first century BC described methods of fastening that were adequately strong, practical and architecturally suitable (Fuchs 2001). However, until the invention of expansion anchors in the early 20th century, anchor technology was restricted, predominantly to casting-in steel or other elements into concrete (Fuchs 2001). As a result of this history, anchor pull-out capacity theory and design approaches for non-homogeneous materials such as clay brick masonry construction have largely been adapted from theory developed for anchoring in concrete (homogeneous) substrates (e.g. Muñoz and Lourenço 2019, Ceroni et al. 2020).

To further understand the reasons for the underperformance of masonry anchors, Burton et al. (2020) conducted in-situ testing of chemical anchors installed centrally within masonry units on three vintage URM residential properties in South Australia. In these tests, brick splitting was the predominant failure mode, and it was observed that an extended softening region occurred over an extended extraction length in which the anchor pull-out capacity remained close to the failure load. This observed failure mode differs from current manufacturer's guidance for the tensile strength design of chemical anchors in masonry (e.g. Powers 2017, Hilti 2019, Ramset 2019). It also differs from the failure models developed through research (e.g. Arifovic and Nielsen 2006, Nielsen and Hoang 2016), which suggest that strength checks should cover failure of the anchor rod, pull-out of the anchor, cone/wedge failures and brick pull-out. Following these checks, application of dimensional restrictions including minimum edge distances are applied to minimise/prevent splitting and spalling, and ensuring that the anchors are correctly installed, with the logical conclusion (Lee and Gad 2017) that incorrect installation will result in underperformance. Importantly, the field-test results of Burton et al. (2020) suggest that splitting failure is a potential failure mode regardless of distance from the free edge or quality of the installation and so the ultimate tensile capacity of chemical anchors in masonry (N_U) can be generalised to

$$N_U = \min(N_{AT}, N_{AP}, N_{CW}, N_{BP}, N_{BS}) \quad (1)$$

where N_{AT} is the ultimate tensile capacity of the anchor rod, N_{AP} is the ultimate pull-out load of the anchor from the masonry unit, N_{CW} is the ultimate load for cone/wedge failure, N_{BP} is the ultimate load for the brick to be pulled out of the wall (failure of the surrounding joints or groups of bricks and joints) and N_{BS} is the ultimate loads required for splitting the brick.

In the remainder of the paper, the mechanism of brick splitting is examined in two ways:

(i) A literature review on existing laboratory and field testing results is conducted, focusing on the types of specimens tested and the test set-up used to identify issues which may result in the prevention of splitting failure.

(ii) A new laboratory test configuration intended specifically to capture the splitting failure mechanism observed in the field tests reported by (Burton et al. 2020) is developed which facilitates simple and inexpensive anchor testing. In addition, the test configuration also captures failure through anchor tensile yield, anchor pull-out and to a limited extent (with

shallow embedment depths), cone/wedge failures. This test set-up which considers wedging and bending stresses within the masonry unit is then used for a comprehensive laboratory campaign considering anchor pull-out capacities (based particularly on masonry unit splitting) under quasi-static, cyclic and impact loading with the quasi-static testing further broken down into tests covering correct and poor quality installation procedures. The influence of unit properties, loading rate, cycling loading and poor installation on anchor performance are then generalised to identify broad implications for the future development of new anchor design approaches which will also include the system response resulting from oscillatory loading from seismic events.

2. Review of previous studies

Let us first consider the failure modes that are assumed to commonly occur in concrete and masonry elements as these have been commonly identified in testing and are the basis of current design approaches:

Anchor tensile yield: Unlike applications with high performance adhesives in concrete substrates where anchor rod tensile failures (Fig. 1a) are a necessary consideration, tensile failure of the anchor rod in clay masonry is unlikely except in the case of deep embedments and small anchor diameters, and as a result is not considered any further here (Arifovic and Nielsen 2006, McGinley 2006).

Anchor pull-out: Pull-out of the anchor rod (Fig. 1b) can be characterised as shear/bond failure at the interface between: (i) the anchor rod and the adhesive mortar; (ii) the adhesive mortar and the masonry unit; (iii) within the adhesive mortar itself; or (iv) a combination thereof; pull-out failure may also feature some localised splitting of the masonry unit. Pull-out failure of the anchor is comparable to the mechanism of the bond strength of reinforcing bars in concrete, with pull-out capacity likely to also be influenced by incorrect or poor anchor installation. In masonry, Nielsen and Hoang (2016) consider this pull-out failure via application of plasticity theory, relating the roughness of the deformed anchor with associated axisymmetric displacement of the base material as a result of the load applied to the anchor and the corresponding bar displacement. Using a more generalised approach, Arifovic and Nielsen (2006) apply plasticity theory to consider sliding failure of bonded anchors in masonry as a function of the strength of the substrate or adhesive mortar, the diameter of the anchor and the depth of embedment.

Cone/wedge failure: When considering cone/wedge failure (Fig. 1c), analysis typically follows that of punching shear failure in concrete assuming the formation of a 45° (or similar) failure cone (e.g. Arifovic and Nielsen 2006, McGinley 2006, Pisani 2016). Unless the mortar strength and the bond strength between mortar and masonry unit is similar to that of the unit itself, (which is generally not the case with clay masonry and lime mortars), masonry is highly non-homogeneous in comparison to concrete. This leads to a truncated cone or wedge type of failure which has been considered in detail by Arifovic and Nielsen (2006) using theory borrowed from anchor failure in concrete.

Unit extraction: Extraction of an entire masonry unit (Fig. 1d), does not involve interaction of the bond between the anchor and the masonry substrate and is not considered further here.

Splitting failure: Design checks for splitting failure (Fig. 1e) in concrete substrates are through strength reduction factors as a function of the distance to free edges (e.g. Hilti 2019), but when referring to masonry, no such reduction factors are available. Predictive models (e.g. Arifovic and Nielsen 2006) have likened splitting in masonry to that of concrete and consider that it is only a phenomenon when edge distances are small and as

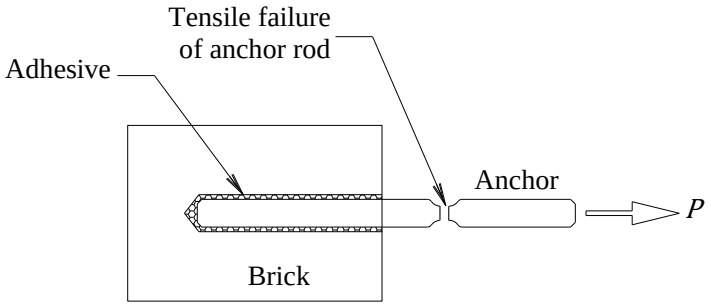

(a) – Anchor rod failure

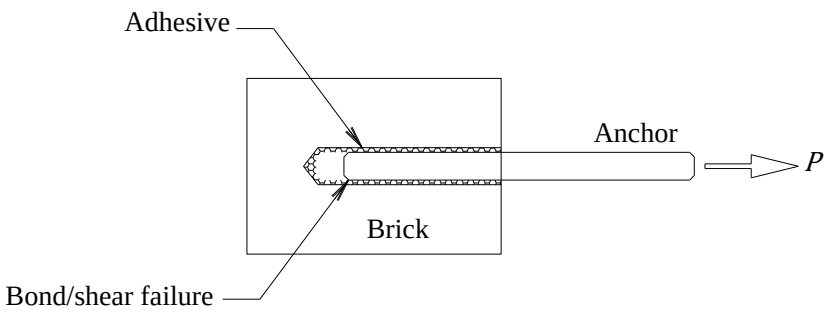

(b) – Bond/shear failure (anchor-adhesive, adhesive-brick and adhesive shear failure

Fig. 1 – Common failure modes

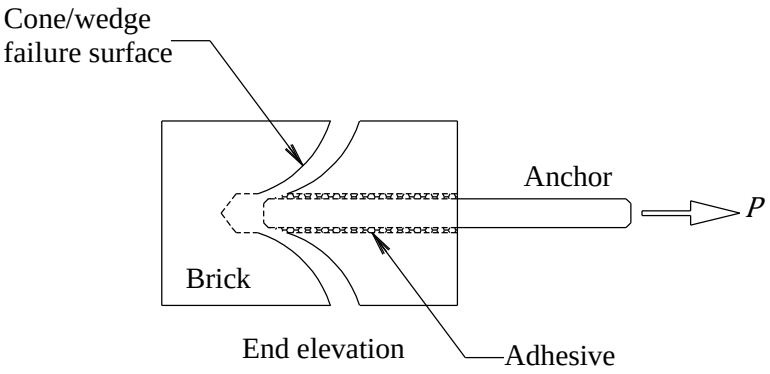

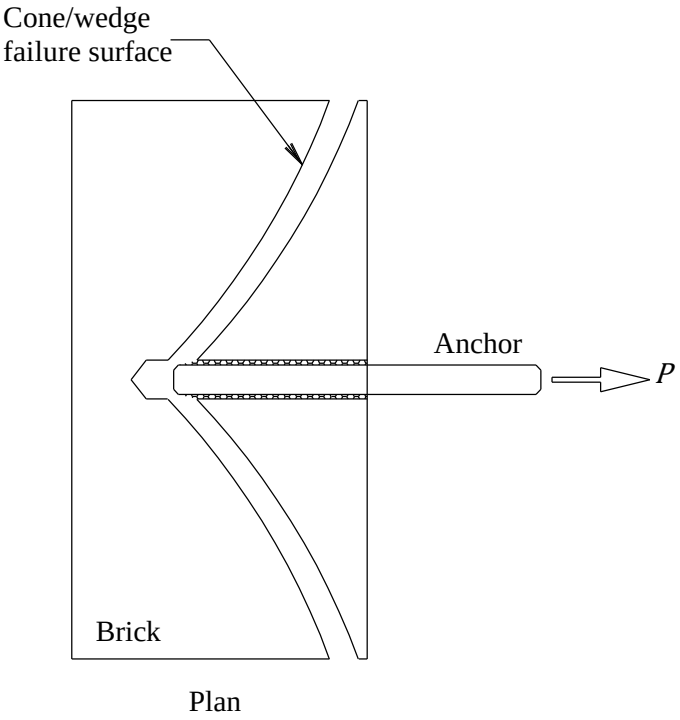

(c) – Cone or wedge type failure

Fig. 1 (continued) – Common failure modes

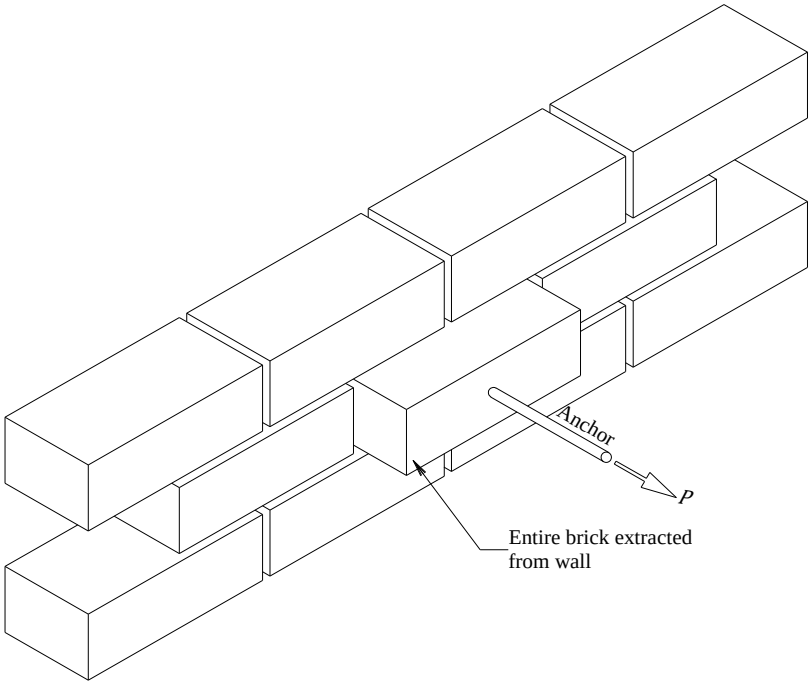

(d) – Extraction of entire masonry unit

Fig. 1 (continued) – Common failure modes

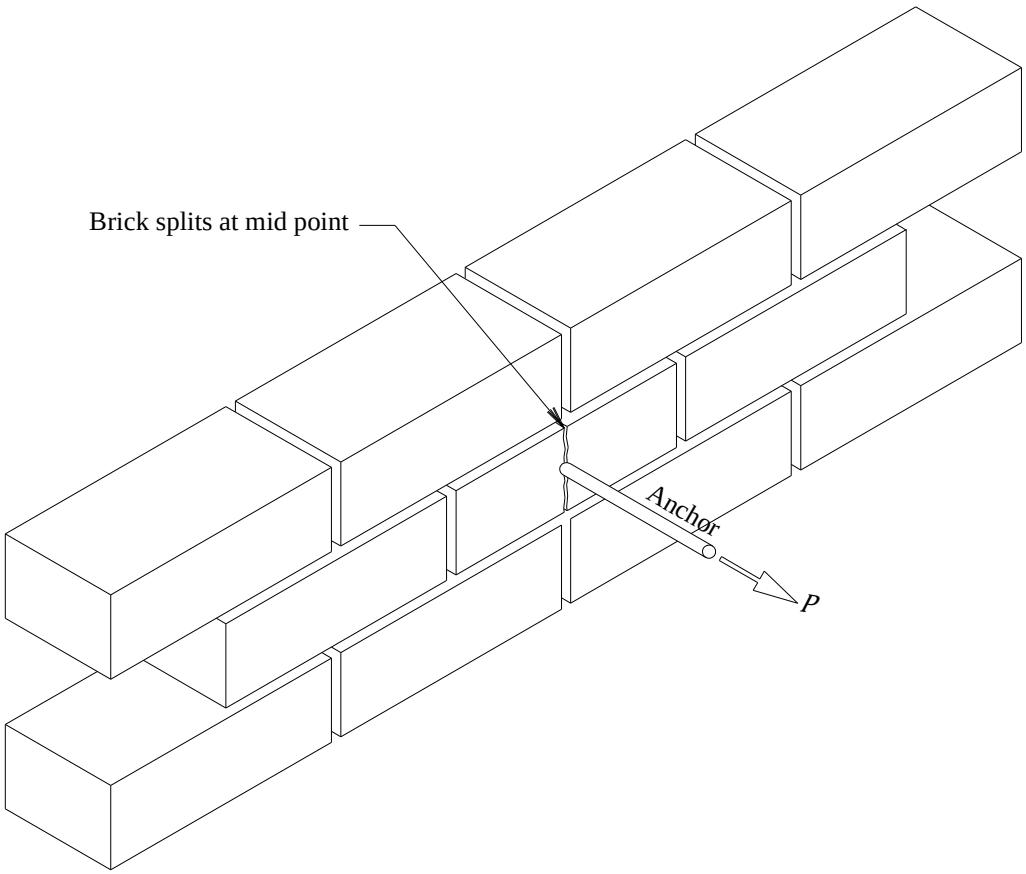

(e) – Masonry unit splitting

Fig. 1 (continued) – Common failure modes

such, splitting failure is assumed to be avoided by placing anchors a sufficient distance from free edges.

A number of experimental campaigns have looked at pull-out capacity of chemical anchors in masonry, covering testing in existing construction and also specifically constructed masonry walls. The nature of the observed failure modes from those campaigns as they relate to the five failure modes discussed above is summarised in Table 1. These experimental campaigns cover a vast array of test configurations with different loading and restraint systems, various anchor sizes and adhesive types and varying depths of anchor embedment. In addition, the tests cover various types of substrates, with some tests conducted on in-situ masonry and others on specifically fabricated laboratory specimens. Therefore, the differences in test configuration are likely to contribute to variations in measured strength and observed dominant failure modes.

With the exception of Giresini et al. (2020) the experimental campaigns shown in Table 1 observed that some brick splitting occurred during the testing that was undertaken. However, with the exception of Burton et al. (2020) it appears that the splitting has been dismissed as a consequence of the adhesive bond failure between the anchor rod and the substrate rather than a specific failure mode, and not considered further. A test configuration that obscures the brick face during (in particular) the early stages of the test as shown in Fig. 2(a) can contribute to this interpretation as the splitting may not be evident until a more obvious failure is reached and the apparatus disassembled. Burton et al. (2020) consider the brick splitting to be a significant (or the principal) contributor to the failure mechanism observed in the tests that they undertook, (rather than being an artefact) as many of the tests resulted in brick splitting being the only observed failure mode. This can particularly be attributed to the depth of embedment of the anchors being tested (in accordance with manufacturer's recommendations) and the masonry geometry (size of masonry unit, location of anchor).

The test studies by Hatzinikolas et al. (1983), Arifovic and Nielsen (2006) and Burton et al. (2020) all load the anchor by reacting against a heavy plate through which the anchor is passed - pulling on the nut to load the anchor (Fig. 2a). This method of connecting the anchor has the disadvantage of obscuring the masonry unit from view during the early stages of the test (when the anchor has displaced minimally) but can accommodate greater anchor displacements with smaller (and lighter) testing equipment. The remaining studies have adopted a direct coupling of a ram to the anchor shown schematically in Fig. 2(b).

Non-uniform tensile stress over the length of the anchor rod (maximum at the face of the masonry unit [the free end], reducing to nominally zero at the maximum depth of embedment) will generate greater strains in the anchor at the free end with the possibility of developing localised failures in the masonry unit at that location. However, Eligehausen et al. (2006) suggest that the bond stress for a single adhesive anchor (in concrete) is best described as uniform over the length of the anchor provided that $4 \leq D_{eff}/d \leq 20$, $d \leq 50\ mm$ and the bonded area $(\pi d D_{eff}) \leq 58E3\ mm^2$ where D_{eff} is the effective depth of embedment and d is the anchor diameter. The limits for validity for 10, 12, 16, and 20 mm ϕ anchors is shown in Table 2. There are significant differences in material strengths and homogeneity between concrete and clay masonry, but the general concept that a uniform stress region exists over varying embedments will remain valid in masonry as it does in concrete. With larger depths of embedment, and the consequent non-linearity of stress along the length of the anchor rod, localised failures such as splitting the outer brick, or localised cone failures are likely to occur. However, these occurrences are likely to be seen as aberrations in the load vs displacement plot

Table 1 – Observed failure modes

Author	Cone/ wedge	Pull out of adhesive "plug"	Bond failure with local brick splitting		Masonry breakout/ anchor pull-out	Yielding of the anchor	Brick pull-out	Comments
			anchor to adhesive	adhesive to brick				
Burton et al. (2020)	Yes[f]		Yes	Yes[g]	Yes			43 in-field tests; adhesive anchors in vintage masonry in three existing buildings; M12 anchors; embedded 80 mm centrally; clay masonry; all anchors located more than three bricks horizontally and two vertically from any free edges
Giresini et al. (2020)	Yes	Yes[a]			Yes		Yes[b]	108 pull-out tests; five types of masonry wall; clay and (AAC) masonry units; cement mortar; epoxy resin adhesive; 10 mm diameter anchors; embedment depths of 90, 120 and 160 mm.
Muñoz and Lourenço (2019)	Yes		Yes[d]	Yes[h]				chemical, mechanical and grout anchors; M10 anchor rods for chemical and grout applications; screw type mechanical anchors
Dizhur et al. (2016)		Yes	Yes		Yes	Yes		nearly 400 in-field tests; straight and bent anchors; embedment depths from 100 to 400 mm; anchor diameters of 12, 16 and 20 mm; epoxy and cementitious grouts.
Miccoli et al. (2015)[c]		Yes[d]	Yes[d]		Yes	Yes	Yes[d]	brickwork and earth block masonry; 10 mm threaded rod in earth masonry; 16 mm diameter rods in brickwork masonry
Arifovic and Nielsen (2006)	Yes	Yes[e]	Yes				Yes	10, 12 and 16 mm diameter anchors; embedded between 90 and 230 mm; clay masonry.
Hatzinikolas et al. (1983)	Yes			Yes				440 adhesive and mechanical anchors; direct tension and shear; clay brick and concrete block masonry

a) referred to as sliding failure in the study
b) similar to "Failure of bond between anchor and adhesive with localised brick splitting"
c) anchor pins in grouted holes used in this study
d) cementitious grout in place of chemical adhesive
e) denoted as sliding failure in this study
f) only one test failed in this manner
g) almost all tests failed in this manner
h) bond failure between adhesive and brick, but no indication of splitting

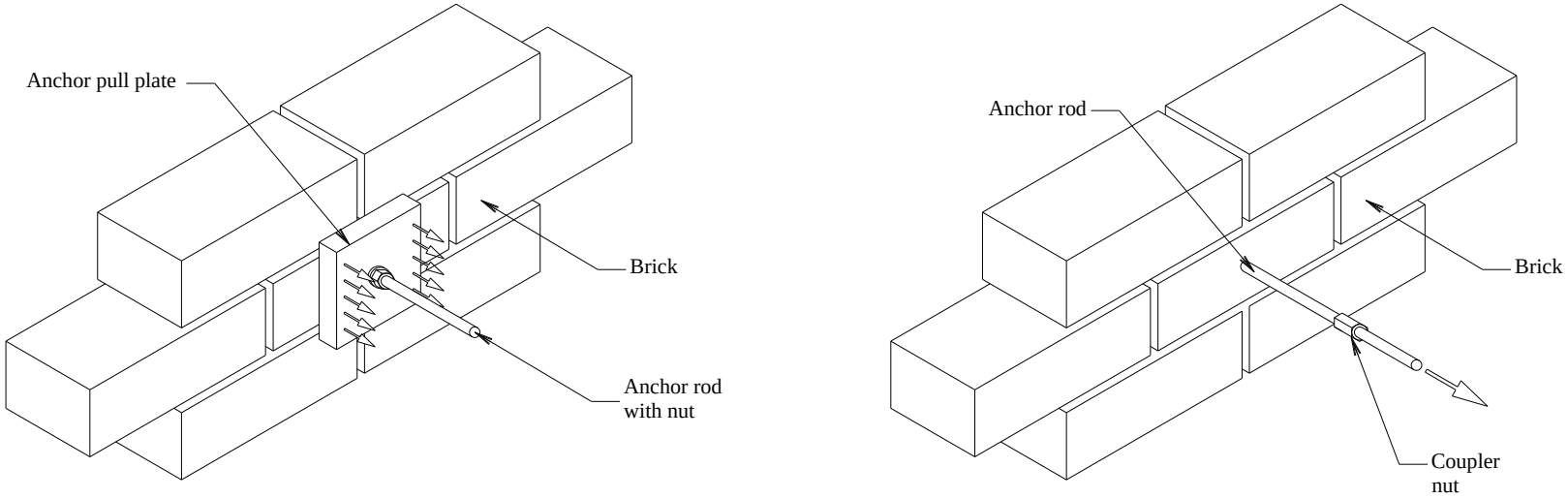

(a) – Pulling plate

(b) – Direct coupling

Fig. 2 – Connection types for anchor pull-out capacity testing

as they are likely to occur below the peak pull-out capacity (POC). In particular, with deeper anchor embedment, the implications of masonry unit splitting having a significant role to play in the overall pull-out capacity are obfuscated as the peak load is likely not to have been reached when the unit splits. As such, the extended softening region, where pull-out capacity remains essentially constant (albeit lower), following failure, as noted by Burton et al. (2020), is not seen. Some of the deeper embedment depths, in particular in the study of Dizhur et al. (2016) for example, are likely to exhibit this behaviour.

Table 2 – Valid anchor embedment depths in concrete for uniform bond stress

Valid embedment depths (D_{eff}) for uniform bond stress in concrete substrate								
	Embedment depths (mm) – lower and upper bounds							
Anchor diameter (mm)	10		12		16		20	
	lower	*upper*	*lower*	*upper*	*lower*	*upper*	*lower*	*upper*
$4 \leq D_{eff}/d \leq 20$	40	200	48	240	64	320	80	400
$\pi d D_{eff} \leq 58E3\ mm^2$	0	1846	0	1538	0	1154	0	923

Further complications with interpretation of results of pull-out capacity and failure mode when large embedment depths are used particularly arise with multi-wythe construction when there is interlocking between courses and wythes. In single wythe construction, the masonry is non-homogeneous with individual units surrounded by mortar of different strength. In multi-wythe construction when there is no cavity, the interlocking of masonry units across wythes, and alternating bonding where, in particular, perpends in one wythe are bridged by the masonry unit of an inner course, creates a situation where instead of individual units transmitting the lateral load to the anchor, a group of units are involved. This will generally increase the failure perimeter, consequently increasing the anchor pull-out capacity more than if a single (equal depth) masonry unit was to be involved with the likely consequence that brick splitting will not be the dominant failure mode. The extent of non-uniform stresses on anchors in masonry as a function of depth of embedment, masonry unit and mortar strengths and masonry unit depth needs further investigation.

Now let us consider the influence of the restraint system adopted in each of the studies summarised in Table 1, particularly in relation to the mode of failure. The restraint provided by the test apparatus is important, because in both field and laboratory testing, the pull-out mechanism involves a combination of stresses arising from: (i) wedge stresses associated with roughness of the drilled hole and friction/cohesion between the adhesive and the hole; and (ii) bending stresses associated with applied load from the anchor and the support condition of the individual brick. Both of these mechanisms contribute to tensile stresses at the face of the masonry unit, and additionally, the stresses can also be impacted by global bending in the wall. Schematic layouts of the restraint systems used in each of the studies are shown in Fig. 3.

When a masonry wall is subjected to out-of-plane loading, depending upon how that load is applied, the wall will be subjected to one-way, or two-way bending and inter-brick torsions as discussed in Vaculik and Griffith (2017). Unless the out-of-plane deflection is significant, the vertical bending component in the wall will have minimal impact on the distribution of any horizontal bending stresses within the masonry unit which is anchored, but the horizontal bending will generate torsional stresses within the brick. These torsional stresses will reduce the internal bending moments if the brick is whole, but will add to the internal bending moment if the brick splits (see Appendix A for a detailed discussion).

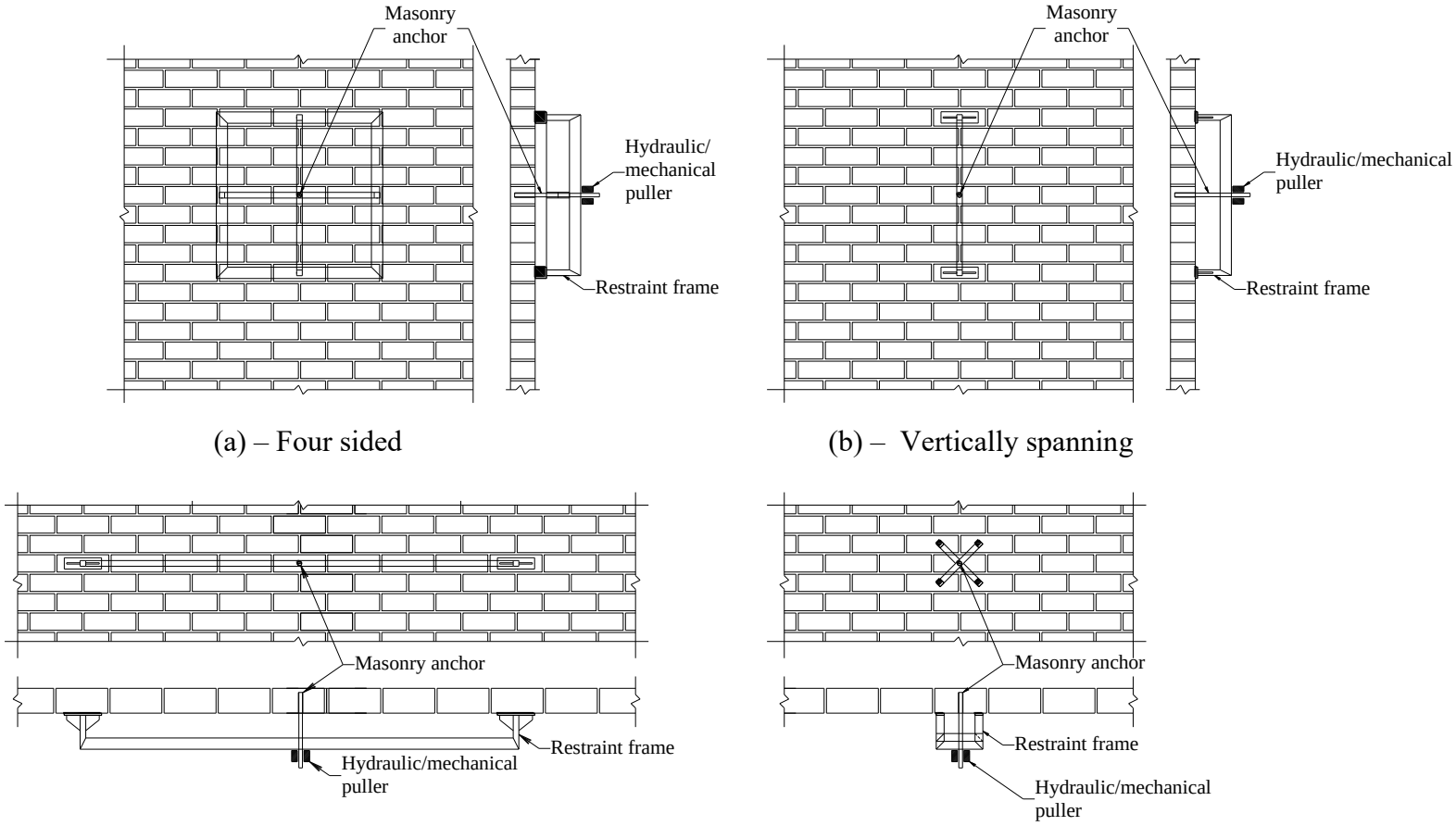

Fig. 3 – Restraint frame systems

The restraint systems that have been adopted by the different studies (Fig. 3) vary in terms of scale, but can generally be categorised as follows:

a) Four sided - The reaction is provided by a frame on all four sides of the anchor as shown in Fig. 3(a). This approach has been adopted by Arifovic and Nielsen (2006), and by Munoz et al. (2018) and results in the masonry within the frame being in two way bending.
b) Vertically spanning – In this configuration shown in Fig. 3(b), a vertically spanning reaction frame reacting against the wall above and below the anchor location is adopted. This method has been used by Hatzinikolas et al. (1983) in which the reaction points are on adjacent bricks, and by Dizhur et al. (2016) in which the reaction points are four to five courses above and below the test location. In this configuration, particularly when there is a large spacing between the reaction points, the wall develops vertical bending, but as a consequence of dimensional compatibility, some horizontal bending is also induced.
c) Horizontal spanning - A horizontal reaction frame as shown in Fig. 3(c) has been used by Miccoli et al. (2015) and Burton et al. (2020). The reaction points are widly spaced in the Miccoli et al. (2015) tests and on units adjcent to the test location for Burton et al. (2020). In this configuration the wall again experiences two-way bending as a result of dimensional compatibility. However, when the reaction points are closely spaced, as was the case with the tests undertaken by Burton et al. (2020), there is minimal deflection within the wall, minimsing horizontal and vertical bending, consequently minimising torsion effects. This short spanning configuration is an improvement over the wider spanning systems and has implications for laboratory testing as discussed in Section 4.2.
d) Close coupled – This configuration used by Giresini et al. (2020) as shown in Fig. 3(d) places the supports in close proximity to the anchor, and therefore is able to minimise both the horizontal and vertical bending moments associated with loading the anchor.

Regardless of the support conditions, it is important to consider that the larger the span of the support system, the greater the (one or two-way) bending and torsional effects within the test region will be, and the influence of greater bending and torsion being that cracking of the wall will impact both the pull-out capacities and failure modes. With the exception of the study undertaken by Burton et al. (2020), the support system span(s) have not been reported, which limits the ability to properly establish the extent of bending contributions. It is also important that the restraint system bears upon the test masonry over sufficient area to ensure that there is adequate distribution of loads, to limit any failure associated with the restraining system.

3. Development of stresses in masonry units during anchor pull-out

Site investigations by Burton et al. (2020) observed that failure of anchorages using chemical anchors in vintage masonry loaded in direct tension was typified by splitting of the brick (refer Fig. 4) rather than a cone or wedge failure. The vertical cracking at the anchor location (mid-length) in the brick is typical of a tension failure caused by horizontal tensile stresses in the brick. These are developed through: (i) wedge stresses associated with roughness of the drilled hole and friction/cohesion between the adhesive and the hole; and (ii) bending stresses associated with applied load from the anchor and the support condition of the individual brick.

3.1. Wedging stresses

Arifovic and Nielsen (2006) suggest that when loading a chemical anchor in a brick, wedge stresses are developed as a result of internal radial compression in the brick, which is induced

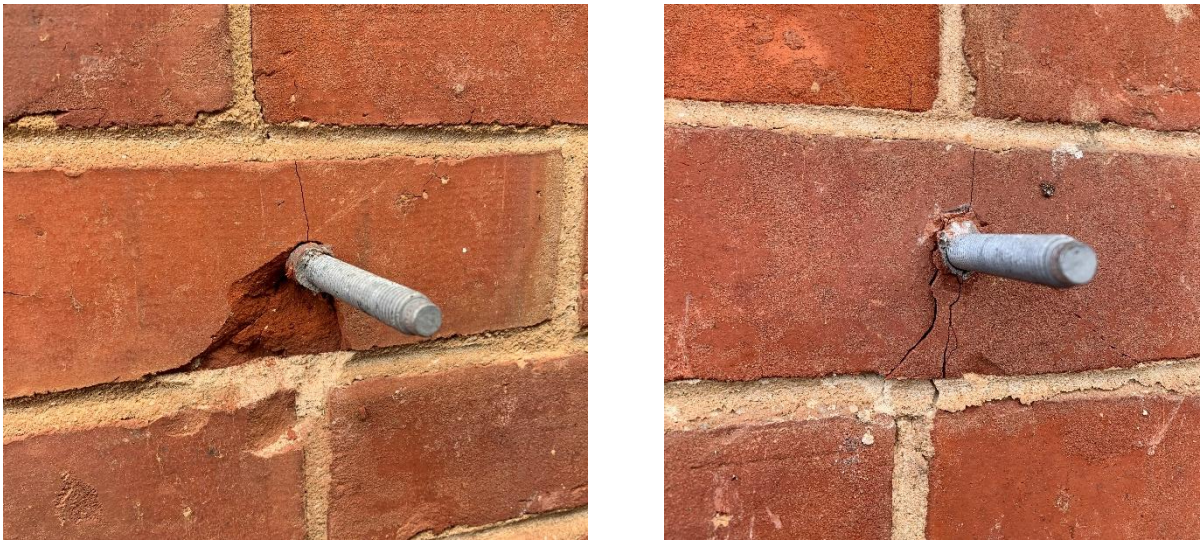

Fig. 4 – Typical anchor pull out splitting failures

by roughness in the drilled hole and the friction plus cohesion between the adhesive mortar and the brick. Firstly, let us examine the wedging mechanism, considering the case where there is no cohesion in order to develop a mathematical model. Initially, consider the wedge and friction stresses by using the simplified two-dimensional wedge in Fig. 5(a). In this scenario, the wedge with a total angle 2θ is forced into the block by applying a load P. The driving force P is resisted by P_t and P_b (acting over the top and bottom halves of the block), which act at an angle of $\theta + \phi$ to the perpendicular, where θ is half the wedge angle and ϕ is the friction angle given by $\phi = \tan^{-1}(\mu)$, where μ is the coefficient of friction between the block and the wedge.

Resolving the forces shown in Fig. 5(b), the splitting force F is

$$F = \frac{P}{2\tan(\theta + \phi)} \tag{2}$$

Extending this two-dimensional case to the three dimensional scenario of a chemical anchor in a drilled hole in a masonry unit involves considering the roughness of the hole combined with the friction between the adhesive and the brick to generate the wedge stresses. Fig. 6(a) depicts the case of a chemical anchor in a drilled hole in a typical masonry unit with the interface between the brick and the anchor enlarged in Fig. 6(b). This represents a "roughness element" between the adhesive and the brick which can be attributable to roughness induced by the action of drilling the hole and voids and hard impurities within the brick creating further irregularities along the drilled surface. The forces acting on the roughness element are shown in Fig. 6(c) (which shows the applied load as $P/2$ as only the lower half of the anchor is being considered), and the forces are then resolved in Fig. 6(d). It is assumed that the roughness elements are distributed randomly throughout the drilled hole. With reference to Fig. 6, and noting that the distribution of bond stresses along the length of the anchor are linear (Eligehausen et al. 2006), development of the wedge forces is independent of the number of roughness elements, or their distribution. That is, the force applied to each roughness element is assumed to be inversely proportional to the number of roughness elements. Thus, in Fig. 6(d), where only one roughness element is depicted, the resisting force is $P/2$. If there were "n" roughness elements

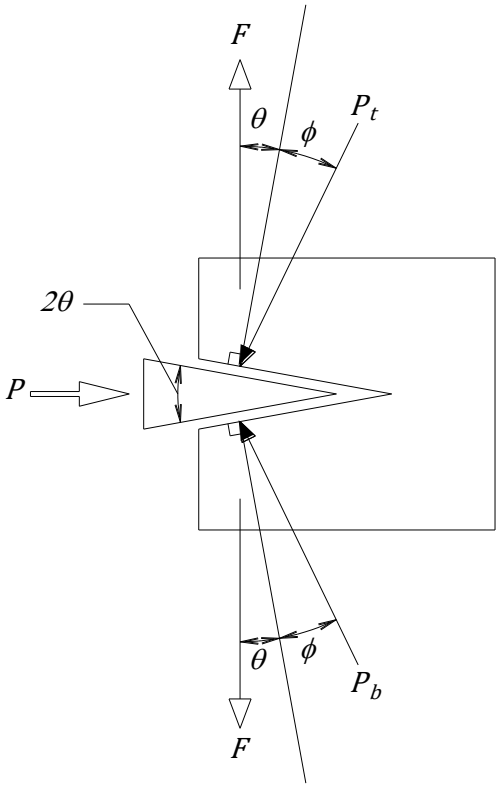

(a) Schematic arrangement

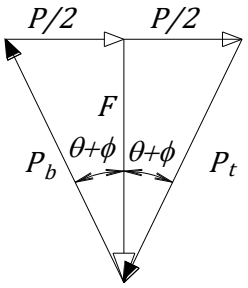

(b) Resolution of forces

Fig. 5 – Two-dimensional wedge forces

shown, the resisting force on each element would be $P/2\,n$. These forces act radially outwards (Arifovic and Nielsen 2006) and are then averaged over the cross section of the masonry.

Arifovic and Nielsen (2006) considered that the surrounding material moves axisymmetrically around the anchor which leads to hoop stresses developing within the base material which can be quantified through thin- or thick-walled theory. Due to the generally non-homogeneous nature of clay masonry, stresses determined through thin walled theory have been used, which are then averaged over an effective cross section of the masonry. Using thin walled theory, the normal force (N) is taken equal to the applied force from the roughness and friction at the interface between the anchor adhesive and the masonry unit. Thus, $N = F_c$ (in Fig. 6d) which is analogous to pressure acting on the drilled surface of the anchor hole so that

$$N = \frac{P}{2\tan(\theta + \phi)} \tag{3}$$

Let us now consider the effect of including the cohesion between the anchor adhesive and the brick. In this model, the contribution of the cohesion to the resistance to the applied load (P_c in Fig. 6) cannot be isolated from the combined cohesion plus friction until the failure load is reached, and the cohesion becomes zero. Thus, when determining the peak failure load, cohesion is included in the model by replacing the friction angle term ϕ in Eq. (3) and in Fig. 6 with the modified term ϕ'. As a consequence, the maximum internal stress generated within

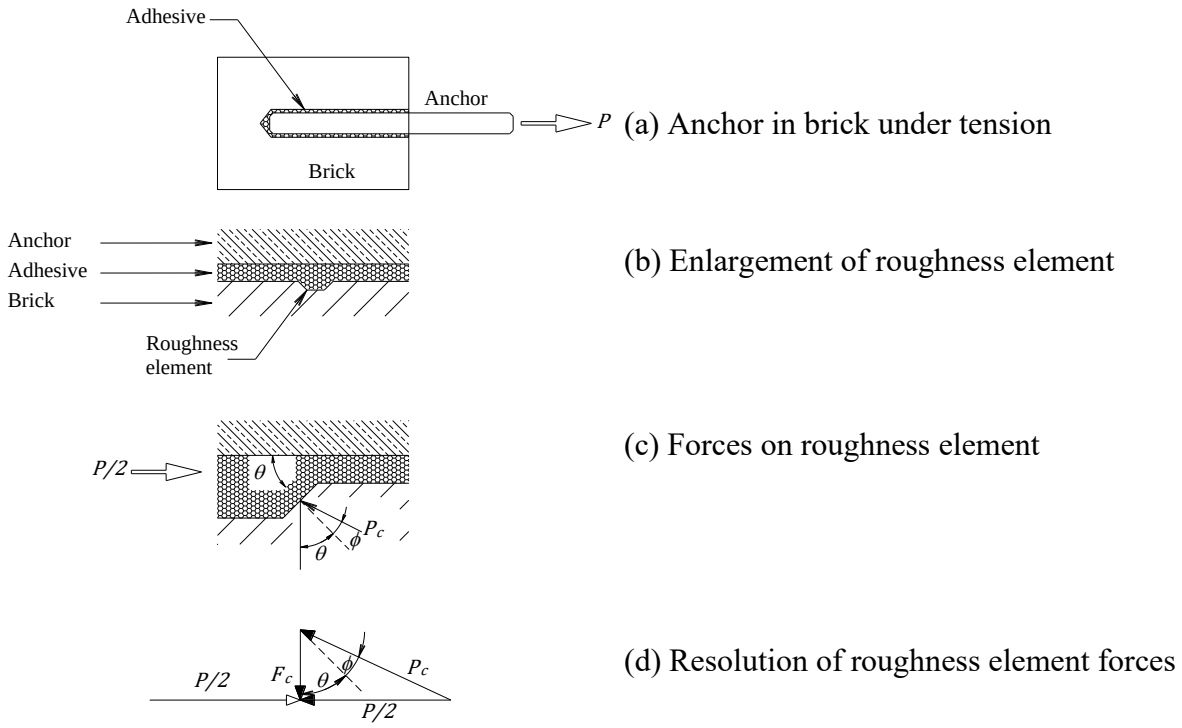

Fig. 6 – Wedge forces from roughness and friction

the brick as a result of the wedge forces (σ_{1-max}) is a function of the normal force (N) and the effective cross section of the brick (A_{eff}) (which allows for influence of anchor embedment depth and any frog), and is given by

$$\sigma_{1-max} = \frac{P}{2A_{eff}\tan(\theta + \phi')} \tag{4}$$

3.2. Bending stresses

The bending stresses that develop within a masonry unit as a result of out-of-plane loads are affected by the support configuration and anchor spacing. In the construction arrangement such as that shown in Fig. 7, the load from the wall is transferred to the anchor through a single brick, which by virtue of how it is built into the wall, is from a uniformly distributed load (UDL) (through friction and cohesion) to the top and bottom faces of the masonry unit. As there is a small but finite vertical distance between the top and bottom faces, there is some minor increase in load transferred on the bottom face of the brick due to the small increase in friction, but this is negligible and can be ignored. There is also some torsion applied to the masonry unit from horizontal bending (see Appendix A) which is not negligible and needs to be considered in design. However, to facilitate comparing site testing and small-scale laboratory test results, it is beneficial to undertake site testing that minimises these torsional effects.

Consider now the stresses that develop in a single masonry unit with an anchor located centrally when the loading is applied as in the study undertaken by Burton et al. (2020), as shown in Fig. 8. Then, as shown in Fig. 9, a load P is applied to the anchor which is resisted by the wall

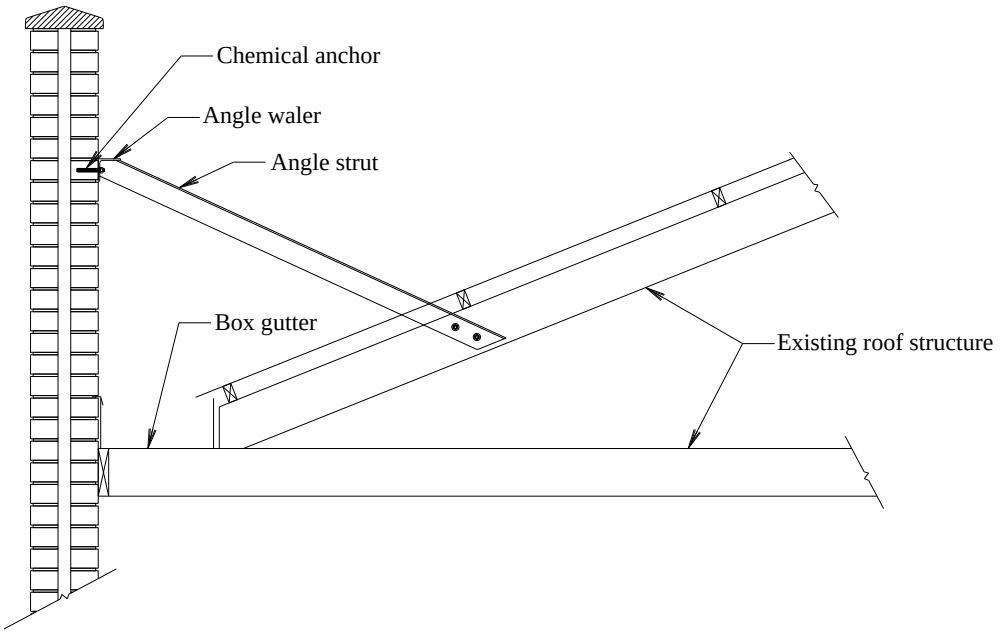

Fig. 7 – Typical parapet retrofit strengthening schematic

through out-of-plane restraining shear forces as shown in Fig. 9(b) which are a combination of cohesion and friction. In this configuration, a Coulomb relationship exists between the cohesion and friction of the form

$$\tau = \tau_0 + \mu\sigma_c \tag{5}$$

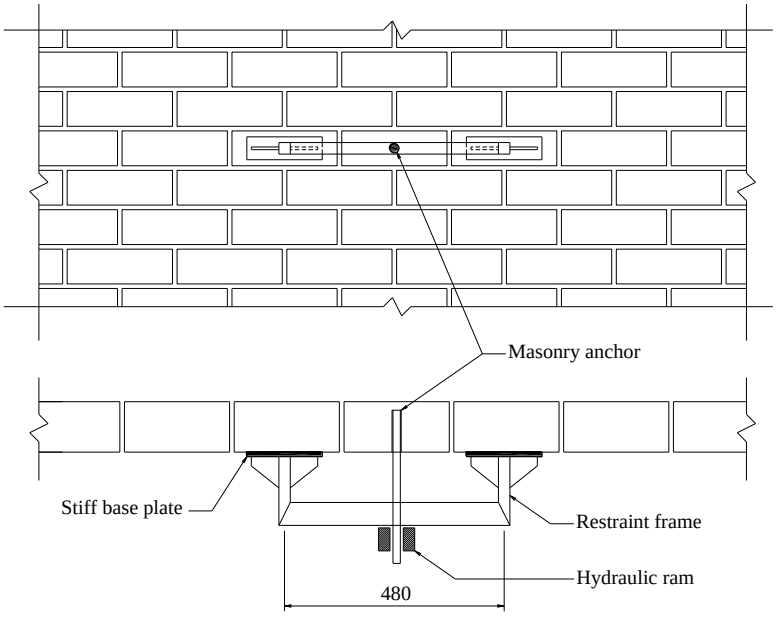

Fig. 8 – Anchor restraint system schematic

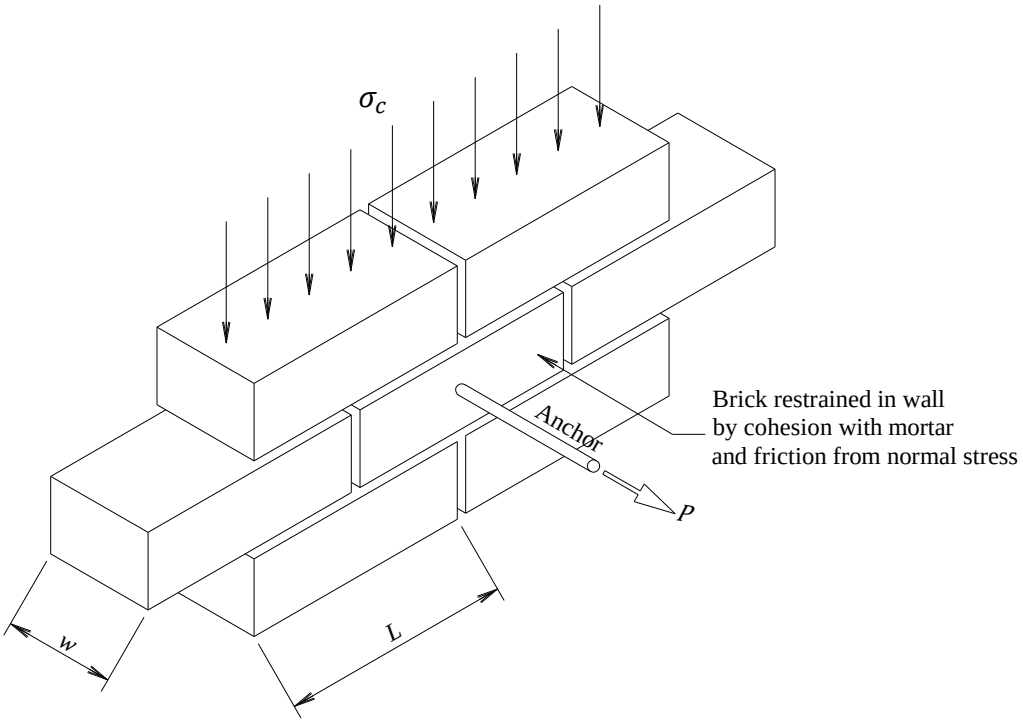

(a) Masonry unit in masonry wall under anchor load

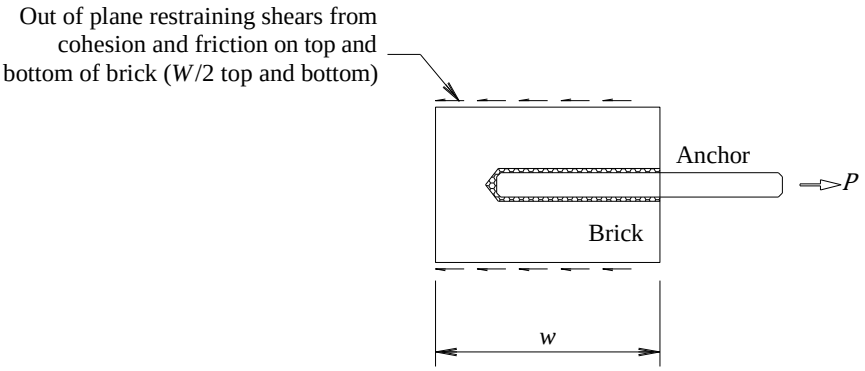

(b) Side elevation of masonry unit showing restraining shear

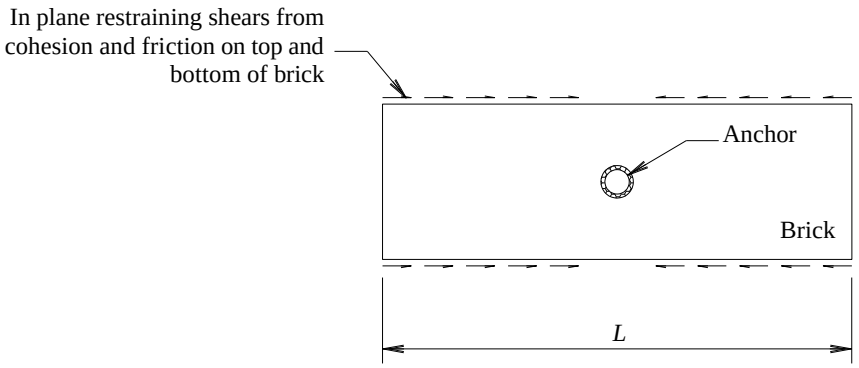

(c) Front elevation of masonry unit showing restraining shear

Fig. 9 – Restraining shear on masonry unit due to cohesion and friction

where τ is the combined shear resistance (from cohesion and friction), τ_0 is the shear strength with zero vertical confining stress, μ is the coefficient of friction and σ_c is the vertical confining stress. In addition to the out-of-plane restraint, there is also an in-plane restraint applied to the brick which provides external restraint to splitting, as shown in Fig. 9(c) and in the same way as for out-of-plane restraint, is a function of friction and cohesion.

In this configuration, the anchor can be considered a point load, located centrally within the brick, and the restraint provided by the brick is a uniformly distributed load over the length of the brick, resulting in a peak bending moment in the masonry unit as shown in Fig. 10 such that

$$M_{max} = \frac{PL}{8} \tag{6}$$

which results in a peak outer-fibre tensile stress of:

$$\sigma_{2-max} = \frac{M_{max}}{Z} = \frac{PL}{8Z} \tag{7}$$

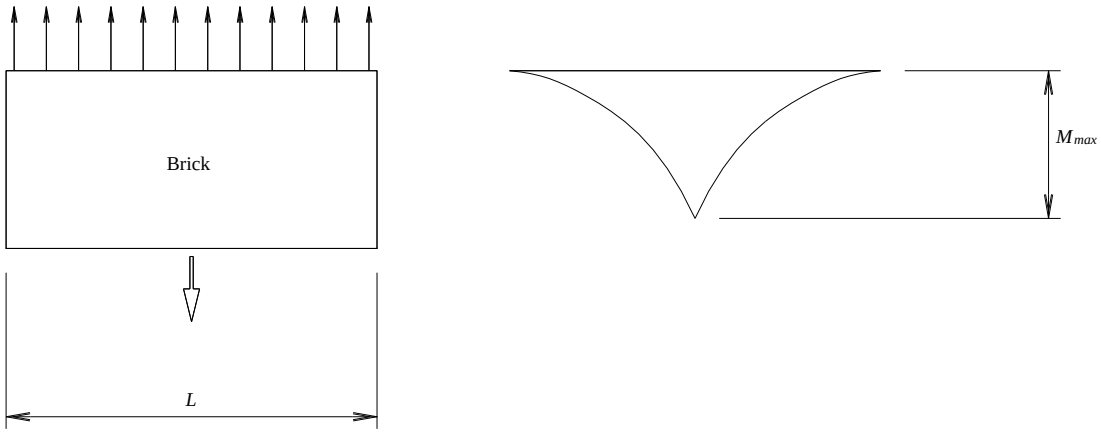

(a) – Loading (b) – BMD

Fig. 10 – Single masonry unit bending moment

3.3. Combined stresses

The wedging and bending stresses combine to develop an outer fibre tensile stress in the brick ($\sigma_{1-max} + \sigma_{2-max}$) which is resisted by the internal tensile capacity of the masonry unit plus the lateral confining restraint as shown in Fig. 9(c). By configuring the on-site testing system such that the torsional component from horizontal bending is minimised by using closely spaced support points, with the support system oriented horizontally, the maximum bending stresses developed in the brick become equivalent to those developed by supporting the masonry unit at quarter points as shown in Fig. 11. Additionally, lateral restraint (denoted P_l in Fig. 11) can then be readily applied to provide the lateral confining resistance. This then provides a simple support system to use in laboratory campaigns allowing for a large number of repeatable tests that cover anchor tensile yield, anchor pull-out and brick splitting failures,

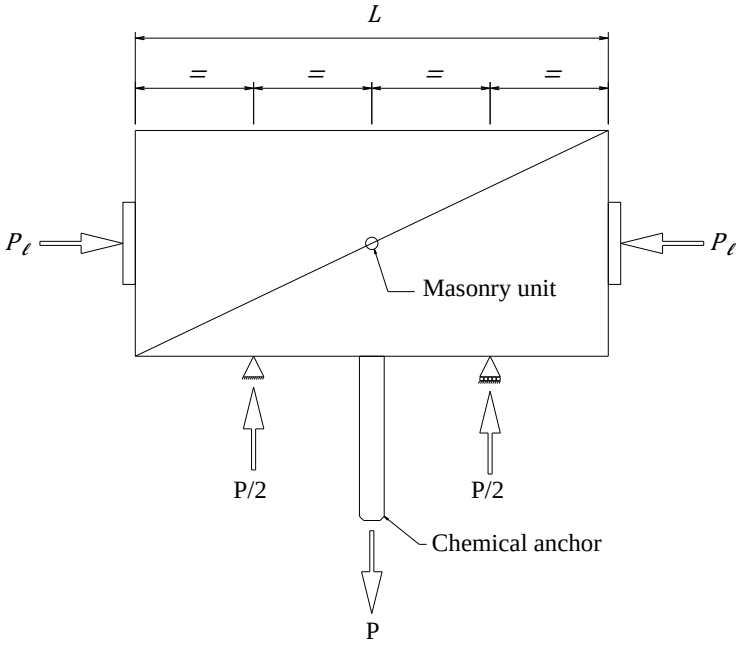

Fig. 11 – Effective support system

with the only limitations being that no vertical confining stress is being applied and that there is a limited ability to develop a cone failure, however, these are considered minor. Using this approach it is possible to perform laboratory testing on single units which have the same support conditions as they would have if located in a masonry wall. This is significant as it allows for testing on single bricks, minimising the need to construct masonry walls in the laboratory environment, which is expensive, and consequently often limits the number of test observations that can be undertaken. It also minimises the need for in-situ testing which is often difficult, firstly because of a lack of availability of suitable structures and secondly because of the damage that would be caused to what are often historically important structures.

4. Test methods

To validate the proposed testing procedure on brick units, the tests reported here were conducted both on plain or frogged units sourced from the same sites as the field testing reported in Burton et al. (2020) and on new units. The new bricks were specifically sourced as moulded (sandstock) rather than extruded units to be similar to the site-won bricks. A typical frogged brick is shown in Fig. 12. Cored or drilled bricks were not used as they are not representative of vintage masonry units due to their geometry and manufacturing process.

The laboratory test program quantifies the material properties (tension and compression) of both the vintage and new masonry units and the anchor pull-out capacities using Hilti M12 zinc plated and galvanised Class 5.8 anchor rods with Hilti HIT-HY 170 injection mortar (a hybrid injection mortar) under quasi-static, cyclic and dynamic loading. In all anchor tests, sufficient adhesive (other than those looking specifically at poor quality installation procedures), was injected into drilled holes 14 mm in diameter and sieves were not used as all the tested units were solid.

4.1. Material tests

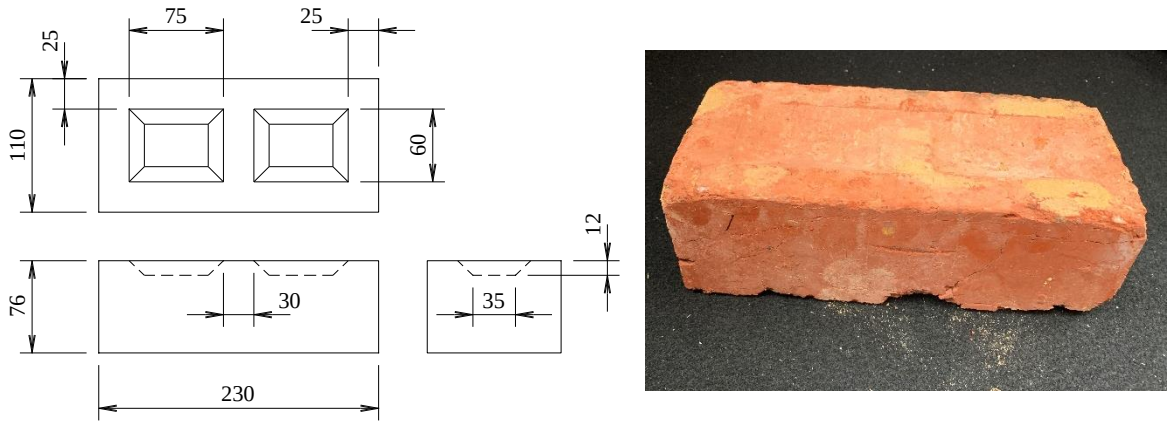

Fig. 12 – Typical frogged masonry unit

4.1.1. Brick tension

Four-point-bending tests were undertaken to determine the flexural tensile strength (also referred to as lateral modulus of rupture) of masonry units, and were conducted following the guidelines of Australian standard AS4456 (Standards Australia 2003). The test configuration that was used is shown in Fig. 13 and the test was conducted at a load rate of approximately 2 kN/minute.

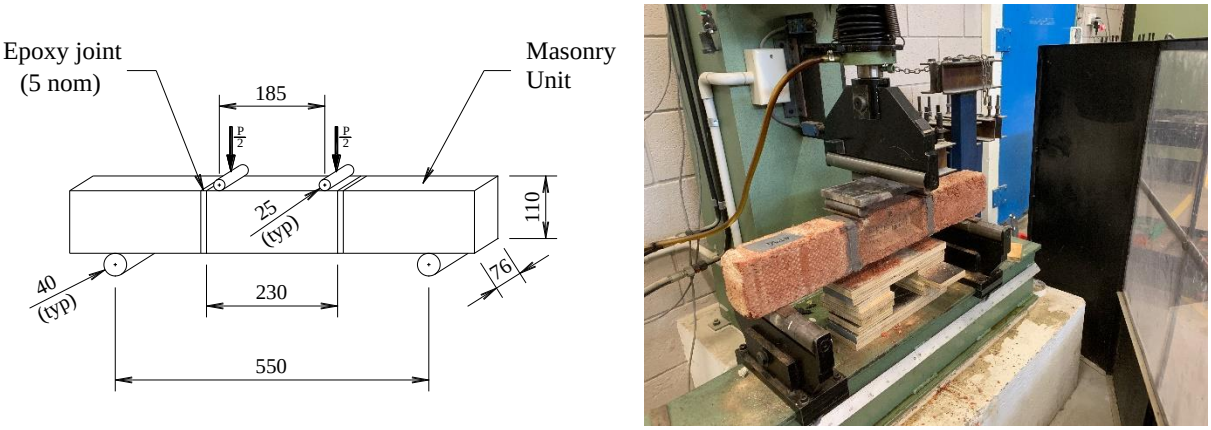

(a) Schematic layout (b) Test apparatus

Fig. 13 – Four point bending flexural tensile (lateral modulus of rupture) test

Direct tensile tests were also undertaken to determine the direct (rather than flexural) tensile strength of the brick samples. For this testing, dog-bone shaped specimens shown in Fig. 14(a) were water-jet-cut from individual masonry units. As shown in Fig. 14(b), the test specimen was subjected to a direct tensile load which is applied at the rate of 2 kN/minute through gimballed clamps to eliminate bending and torsional effects.

4.1.2. Brick compression

Compression tests on brick specimens were used to determine the compressive strength of the individual brick units rather than the masonry as a whole. To achieve this, specimens were

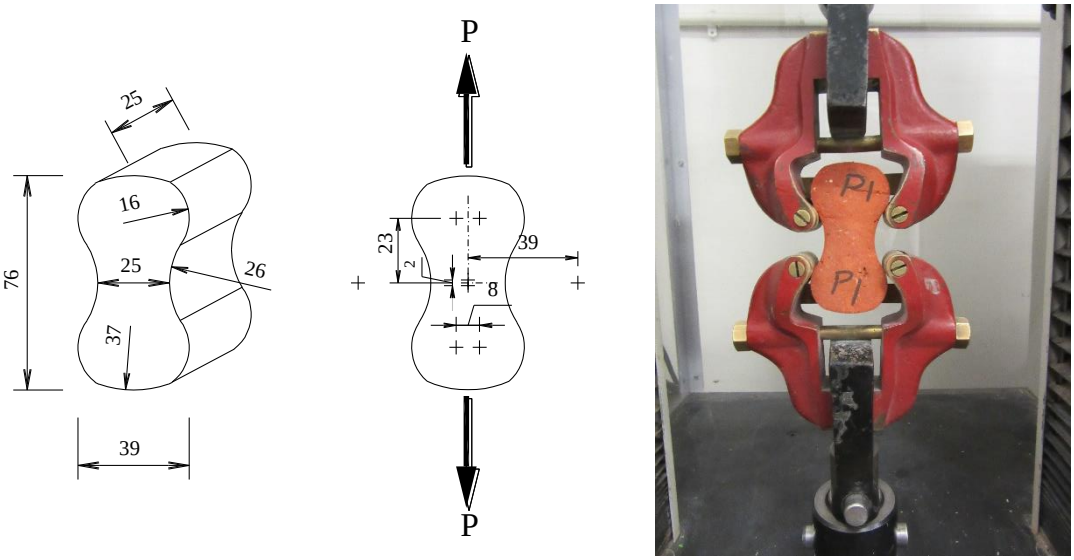

(a) Schematic layout (b) Test apparatus

Fig. 14 – Dog bone direct tensile strength test

saw-cut from individual masonry units with the "long" axis of the cut specimen being parallel to the height dimension of the parent brick, with an average length to width ratio of 3.4:1. These test specimens were then loaded at approximately 2 kN/minute in the configuration shown in Fig. 15 until failure. As the range of brick units included frogged and unfrogged configurations, and that there was considerable variation in the dimensions of the frog, testing of whole units (whether the frogs were filled or not) would lead to strength variations based on

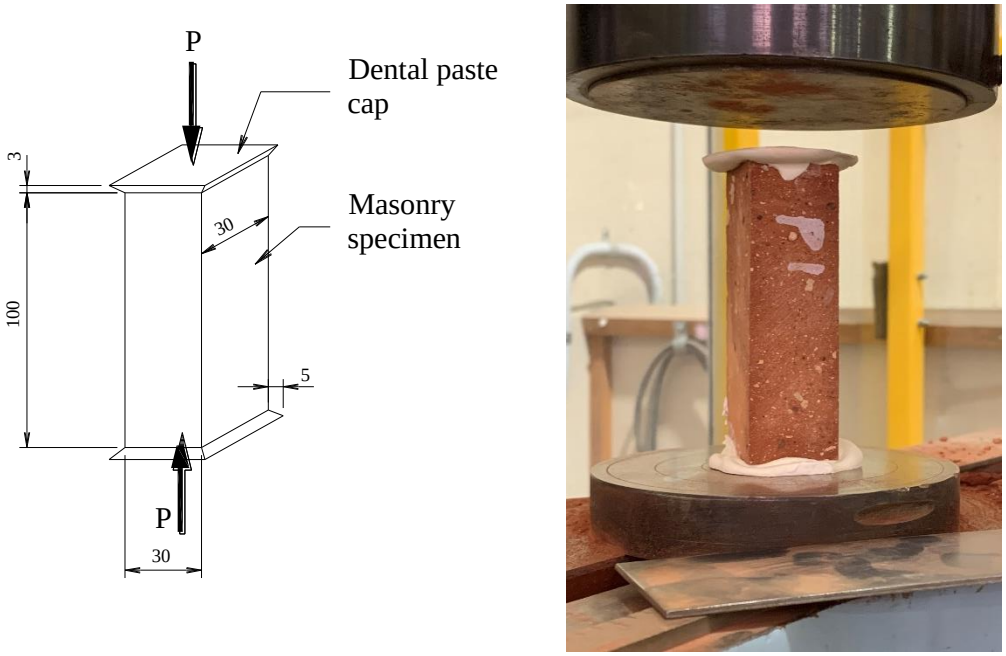

(a) Schematic layout (b) Test apparatus

Fig. 15 – Brick unit compression strength test

the brick geometry. For this reason, saw-cut specimens of the same shape and size were used. Brick compression strength is not directly applicable to anchor pull-out capacities reported in Section 5, but the tests have been undertaken to allow comparison to other available data sets.

4.2. Anchor testing

Three basic test types have been undertaken to determine the pull-out-capacity of chemical anchors which cover: (i) quasi-static tests with both correctly installed anchors and also anchors which have been installed where manufacturer's guidelines have not been followed (poor installation); (ii) impact tests where the anchor has been subjected to high rate impact loading and; (iii) cyclic loading where load- and displacement-controlled cycling has been undertaken. All three test types were undertaken using the support system shown in Fig. 11 other than for the impact tests, which did not incorporate a lateral confining load (P_l).

4.2.1. Anchor support system

Before undertaking the pull-out-capacity tests, it is necessary to quantify the level of lateral confinement (P_l) required to simulate in-service conditions. Cohesion and friction combine in a masonry wall to provide resistance to shearing of individual masonry units, both out-of-plane (Fig. 9b) and laterally within the wall (Fig. 9c). With the support system that has been adopted as shown in Fig. 11, there is no requirement to hold the masonry unit "in place", but it is necessary to determine the correct value of P_l to provide the lateral constraint that contributes to the "available tensile capacity" of the brick. Here, the lateral resistance (τ) is equal to the shear strength of the mortar joint plus the friction component, such that $\tau = \tau_0 + \sigma_c$. In terms of the overall support system (in- and out-of-plane) shown in Fig. 11, P_l provides this lateral resistance (which is the major component enabling the extended softening region during anchor extraction which was seen in the in-situ tests reported by Burton et al. (2020)), and consequently it is important that it is correctly applied in laboratory experimentation to enable the extended softening to be replicated.

AS3700 (Standards Australia 2018) suggests that the characteristic shear strength (f'_{ms}) of masonry should be taken as not less than 0.15MPa, and not more than 0.35MPa which is the equivalent of τ_0 in Eq. (5). As vintage masonry is often associated with lower strength lime mortars, a "typical" value of f'_{ms} (τ_0) of 0.2MPa has been considered, and ignoring contribution from perpends and friction (σ_c is generally small compared to f'_{ms}), the notional lateral confining resistance P_l is given by

$$P_l = 2\tau\left(\frac{A_B}{2}\right) \tag{8}$$

where A_B is the bedded area of the brick ($L \times w$ in Fig. 9a) and in this case

$$P_l = 2 \cdot 0.2\left(\frac{A_B}{2}\right) = 5.06kN \tag{9}$$

Thus, in the absence of contributions from perpends and friction and using $f'_{ms} = 0.2MPa$, a value of P_l of $5.06kN$ could be considered as an upper bound to the available lateral confining resistance, but could be less (or more). To test the notional lateral confining resistance P_l determined in Eq. (9), a series of 22 quasi-static anchor pull-out tests on new masonry units using differing lateral confining loads and supporting the brick either with or without bending were undertaken. During in-service loading, the anchorage is always loaded via the masonry "pulling away" from the support structure developing both bending and wedging stresses.

During initial installation and tightening of the anchor, if the support structure is in direct contact with the brick in which the anchor is installed, then there are minimal bending stresses developed. If there is a gap between the support and the anchor, then bending stresses also are developed during installation. Testing with and without bending was undertaken to compare the strengths in these two scenarios. The results of these tests are shown in Table 3 and the load-slip data is reported in Appendix B. As expected, the tests with no lateral confinement exhibited no extended softening as the brick fractures once the peak load is reached. The tests that used confining resistances of 2, 5 and 10 kN exhibited extended softening, although not in all cases when 10 kN was used. For tests with 15 kN of confinement, no extended softening region was observed and the failure was characterised by brick fracture.

Table 3 – Confining resistance (P_l) validation

Test label	Test Number	Support configuration with bending (W) no bending (N)	Lateral confining resistance P_l (kN)	Anchor peak pull out capacity (kN)	Extended softening region Yes (Y) No (N)
CH5GM12	5	N	0.0	7.86	N
CH6GM12	6	N	0.0	7.31	N
CH3GM12	3	N	2.0	13.26	Y
CH2GM12	2	N	5.0	17.97	Y
CH12GM12	12	N	10.0	16.10	Y
CH4GM12	4	N	15.0	22.71	N
CH1GM12	1	W	0.0	7.94	N
CH11GM12	11	W	0.0	9.58	N
CH13GM12	13	W	0.0	9.25	N
CH18GM12	18	W	0.0	8.80	N
CH9GM12	9	W	2.0	6.91	Y
CH14GM12	14	W	2.0	9.59	Y
CH19GM12	19	W	2.0	8.94	Y
CH8GM12	8	W	5.0	11.01	Y
CH15GM12	15	W	5.0	12.43	Y
CH20GM12	20	W	5.0	11.29	Y
CH7GM12	7	W	10.0	13.39	N
CH16GM12	16	W	10.0	14.33	N
CH21GM12	21	W	10.0	17.64	Y
CH10GM12	10	W	15.0	12.76	N
CH17GM12	17	W	15.0	16.14	N
CH22GM12	22	W	15.0	19.77	N

C ⇒ *Chemical anchor*
H ⇒ *Hilti HIT-HY 170 injection mortar*
G ⇒ *Good (new bricks and good quality installation*
M12 ⇒ *M12 threaded rod anchors*

A series of three separate tests were undertaken applying axial load only to individual masonry units to check that the result using the 15 kN P_l was not influenced by overloading the brick. These tests were undertaken in a compression testing machine by orienting the brick vertically (Fig. 16) between spherical seat platens with load distribution plates configured in the same

manner as with the lateral restraint (P_l). The results of these tests are shown in Table 4. The average failure load of 29 kN is significantly greater than the applied 15 kN, indicating that over confining the test unit laterally was not a contributing factor. It is surmised that the fracturing which occurred when the 15 kN lateral confinement load was adopted (a typical failure is shown in Fig. 17) is a result of impulse propagation through the brick resulting from the rapid energy released at failure, causing instability within the masonry unit.

Table 4 – Lateral failure load test for new bricks

Lateral failure loads	
	Failure load (kN)
Test 1	32.5
Test 2	23.6
Test 3	31.1
Mean	29.0
Standard deviation	4.8
C of V	0.17

Global deflection of masonry units during in-situ anchor extraction tests results in a larger anchor displacement with increasing load than is seen in the laboratory tests undertaken here, as is evidenced in the load/slip plots shown in Appendix B, where the anchor displacement at peak load for the typical in-situ test is considerably greater than the laboratory results. Masonry variability precludes obtaining exact matches for strengths and displacements, but using 5 kN

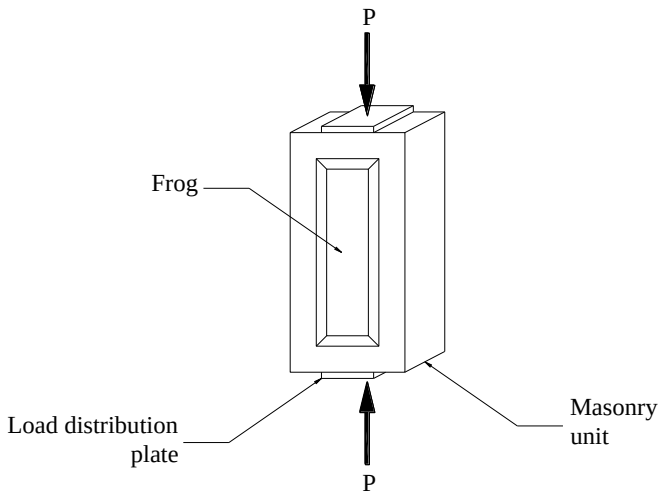

Fig. 16 – Schematic layout of masonry unit axial load test

lateral confining resistance has resulted in a good match for peak pull-out capacity and extended softening. This possibly suggests that the mortar shear strengths at the sites where the in-situ tests were conducted had an upper bound of approximately 5 kN. As this value matches the notional theoretical confining resistance from Eq. (9) it was adopted for all subsequent quasi-static and cyclic anchor pull-out tests.

Fig. 17 – P_l test specimen (CH17GM12) fracture

Simulation of in-situ masonry conditions is always difficult in the laboratory even when full-scale testing is undertaken, as the time history of loading and thermal variations combined with variations in quality of manufacture, quality of materials and actual mortar mixes impacts the results. However, as shown in the load/slip plots in Fig. 18, which show the typical in-situ unit load slip curve, (which has been adjusted to "remove" the test apparatus and initial system deflection but keep the global masonry deflection), and the laboratory tests which utilise the 5kN lateral resistance, there is good agreement between the two.

4.2.2. Quasi-static testing

The quasi-static tests were all undertaken using a manually driven worm gear drive loading apparatus that was horizontally oriented as shown in Fig. 19(a). This type of machine was specifically used in a hand operated format to avoid under- or over-shooting of target loads that might occur with hydraulically operated equipment and also to avoid load cycling during hydraulic pump cycles. Anchor displacement was measured with a single 100 mm LVDT (linear variable differential transformer) measuring total anchor displacement and three 10 mm

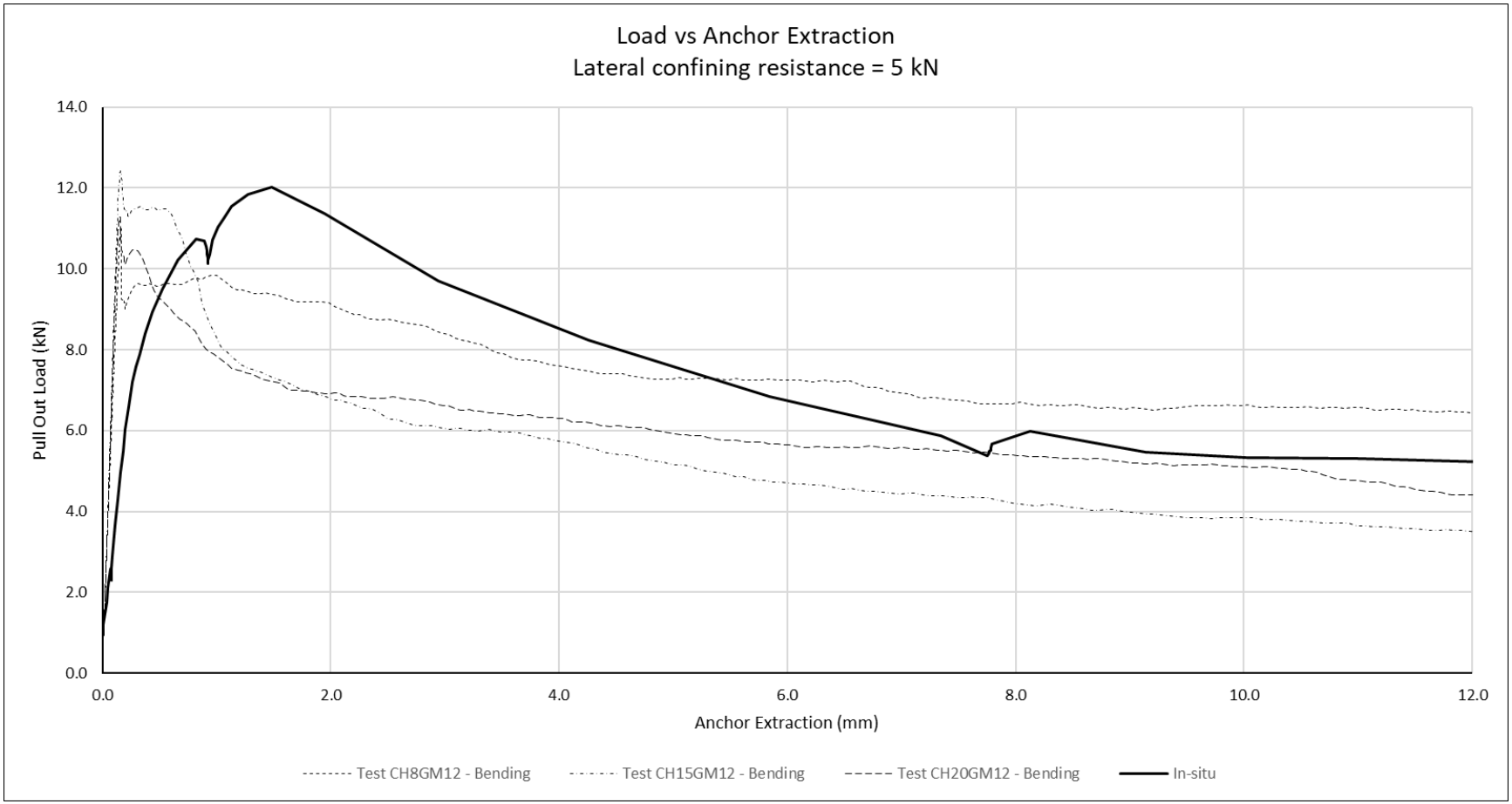

Fig. 18 – P_l validation tests – load vs displacement

(a) – Mechanical pull test rig

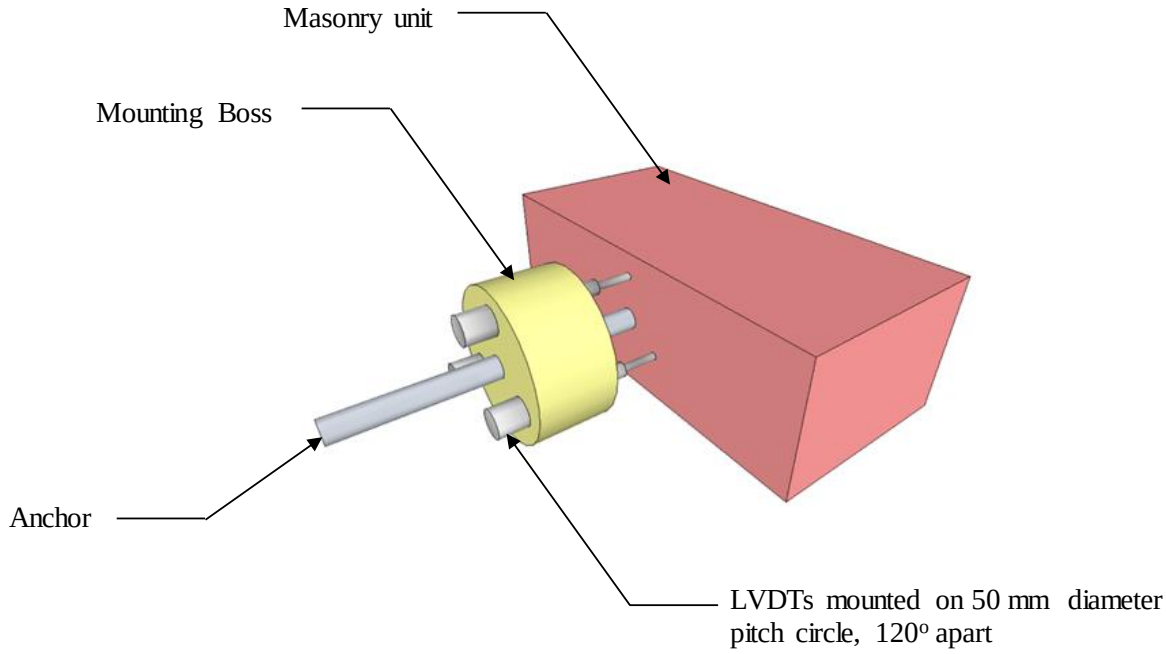

(b) – Mounting boss layout

Fig. 19 – Anchor test setup

LVDTs arranged circumferentially around the anchor at 120° in a mounting boss that was clamped to the anchor (shown pictorially in Fig. 19b) directly reading anchor displacement against the brick on a pitch circle diameter of 50 mm, to avoid impact of localised spalling around the anchor. In addition, a 10 mm LVDT was used to measure displacement of the LVDT mounting boss relative to the reaction frame (supports). The lateral confining load was applied using a steel restraint frame with a threaded clamping mechanism acting against steel platens at either end of the brick, which was free to move with the test unit, and the applied load was measured with a cylindrical load cell with a maximum load capacity of 50 kN. Adjustment of the lateral confining load during testing is able to be made through adjustment of the clamping mechanism, although it is expected to not be required as any increased lateral load will be offset by reduced compressive loads within the unit. A general arrangement of the

instrumentation configuration is shown in Fig. 19(c). These tests were conducted on old and new masonry units covering correct and incorrect installation procedures to study the sensitivity of anchor capacity to installation variability as detailed in Table 5 with the incorrect procedures being those identified as most likely to occur on site. Combinations of poor or incorrect installation practices were not considered as it is expected that experienced technicians will be engaged for this type of work on site, and errors will be a result of inattention or distraction rather than malicious intent. All the quasi-static tests used a lateral confining resistance (P_l) of 5 kN.

4.2.3. Impact testing

Although some chemical anchor manufacturers do not provide seismic design guidelines, anecdotal evidence (based on the Australian experience) suggests that many of these products are nonetheless used for seismic application. To determine whether high rate loading adversely affects the pull-out capacity of chemical anchors, tests using high rate impact loading were carried out using the Hilti anchors as noted above (which are not approved by Hilti for seismic loading) (Hilti 2019). The impact tests were undertaken using accelerations significantly greater than those that could be expected during seismic events so that interpolation between these and the quasi-static test results would cover any possible seismic accelerations.

Two series of tests under impact loading were undertaken using a swinging hammer machine manufactured for this project. The machine, which is shown in Fig. 20 configured with a total hammer mass of approximately 5.6kg, has an impact speed of approximately 4.1m/s. This results in an impact energy of approximately 50J to the anchor with an associated anchor acceleration of approximately 5000ms^{-2}. A 50 kN cylindrical load cell was used to determine the pull-out-load and was poled at a rate of 50,000 samples per second to be confident of measuring the peak anchor load from the impact.

Due to the high sampling rate considered necessary to capture the peak load, a load cell was used rather than an accelerometer which meant that the dynamic mass of the test apparatus needed to be deducted from the measured peak anchor failure load. To achieve this, impact testing was conducted in two series: the first was undertaken using new bricks that were simply supported with no lateral confining resistance in the configuration shown in Fig. 11, with $P_l = 0$. The second series used "bricks" made from expanded polystyrene with anchors installed in the same manner as was used for the new bricks with the polystyrene brick being used to provide support to hold the anchor in-place, but not to restrain it against the applied load. These tests were undertaken to estimate the dynamic mass of the anchor, load cell and anchor assembly to enable the acceleration forces on these elements to be deducted from the brick test results. It was not practical to apply the confining resistance to the polystyrene "bricks" and so both these series of tests were conducted without confining resistance, and whilst this is likely to slightly underestimate the impact pull-out capacity, it was considered to be conservative and a suitable "trade off" to keep the two test configurations the same.

4.2.4. Cyclic testing

Load-controlled and displacement-controlled tests on new bricks were undertaken with the same support configuration that was used for correctly installed anchors using a lateral confining resistance P_l of 5 kN. The load-controlled tests involved three cycles each from no-load to $1/3$, $2/3$ and $3/3$ of the expected failure load and extended in $1/3$ (of expected failure load) increments until failure occurred. The displacement-controlled tests used the same configuration as the load controlled tests, but with three cycles each from zero displacement to

Table 5 – Quasi-static anchor pull out tests

Quasi-static anchor installations									
All anchors M12 class 5.8 threaded rod with Hilti HIT-HY 170 injection mortar without the use of sieves									
Installation methodology	Series name	Brick type	Hole depth (mm)	Anchor embedment (mm)	Installation quality		Tests performed		
					Hole cleaning[1]	Mortar injection	Quasi -static	Cyclic	Impact
14mm ϕ hole drilled 80mm deep into brick, correctly cleaned with correct volume of injection mortar	*correct*	*old and new*	80	80	*normal*	*full*	Y	Y	Y
as per "*correct*" but hole depth only 40mm	*short hole*	*new only*	40	40	*normal*	*full*[2]	Y		
as per " *correct* " but hole drilled completely through brick allowing mortar to spill out behind	*long hole*	*new only*	110	80	*normal*	*full*[3]	Y		
as per " *correct* " blown out without being brushed out	*not brushed*	*new only*	80	80	*blown only*	*full*	Y		
as per " *correct* ", brushed out but not blown out	*not blown*	*new only*	80	80	*brushed only*	*full*	Y		
as per " *correct* " but no cleaning at all	*not cleaned*	*new only*	80	80	*none*	*full*	Y		
as per " *correct* " but only half the required mortar injected	*half filled*	*new only*	80	80	*normal*	*half*	Y		

1 normal = brushed and blown clean

2 adequate mortar used but only half that of a full depth hole

3 adequate mortar to fill the hole, but considerable volume escaped through the hold through the back of the brick

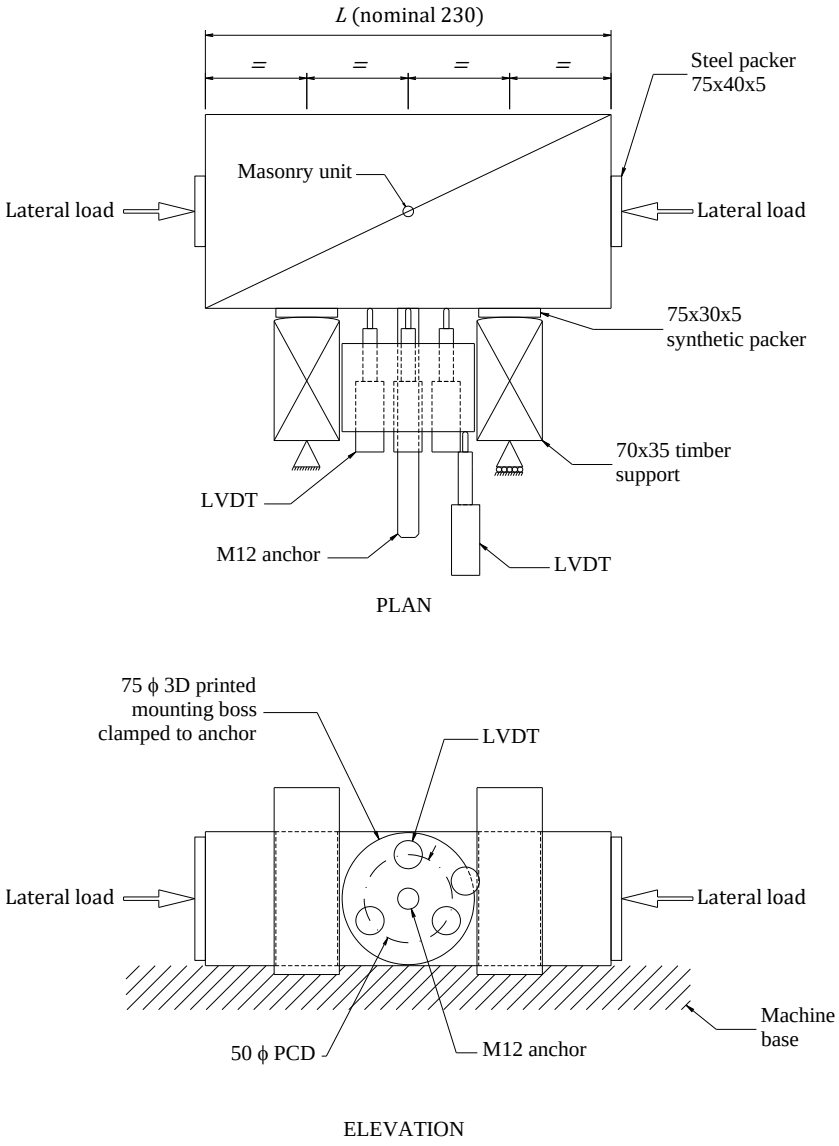

(c) – General arrangement

Fig. 19 – Anchor test setup (continued)

1/3, 2/3 and 3/3 of the expected failure displacement and was continued following failure to observe changes in load capacity. Only a single load controlled and displacement controlled test was undertaken (on new bricks) as it was expected that due to the observed extended softening region the cyclic loading would have minimal impact on the load capacity over time but exhibit ongoing hysteresis with each cycle.

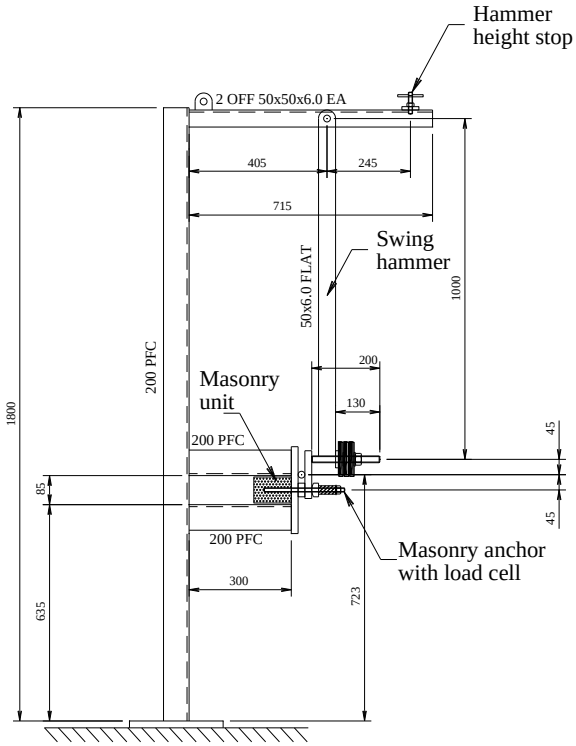

(a) Schematic layout

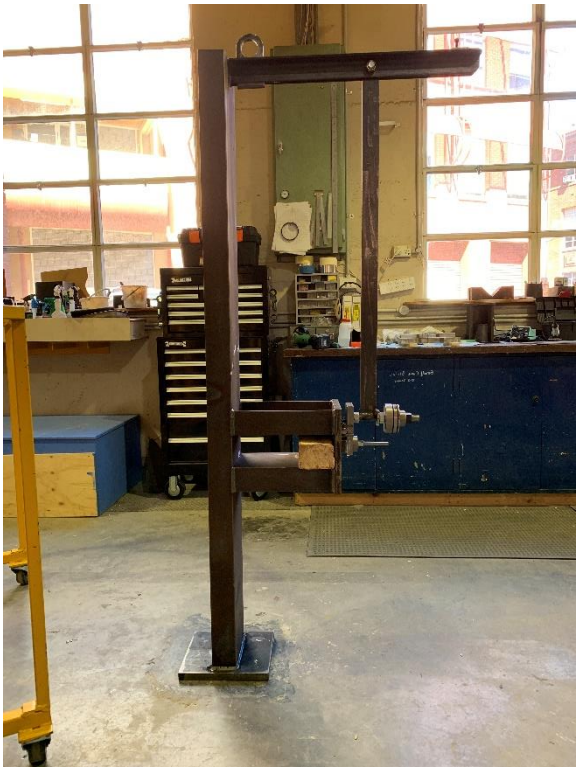

(b) Test apparatus

(c) Loading system

Fig. 20 – Impact load test machine

5. Results

5.1. Material testing

Flexural tension

Mean flexural tensile strength of the site-won bricks varied from 1.83 to 2.02 MPa with coefficient of variation between 0.28 and 0.43. The mean for the new bricks was 2.89 MPa with a coefficient of variation of 0.03. The results for these tests are shown in Table 6.

Table 6 – Masonry unit properties

Masonry unit properties – Croydon park and new bricks				
	M	P	S	N
Flexural tension				
number of tests	4	4	4	4
mean stress at failure (MPa)	1.94	2.02	1.83	2.89
standard deviation (MPa)	0.54	0.82	0.78	0.08
coefficient of variation	0.28	0.41	0.43	0.03
5th percentile stress at failure (MPa)	0.7	0.1	0.0	2.7
Direct tension				
number of tests	6	6	6	12
mean stress at failure (MPa)	1.68	1.60	1.98	1.40
standard deviation (MPa)	0.63	0.39	0.52	0.37
coefficient of variation	0.37	0.25	0.26	0.26
5th percentile stress at failure (MPa)	0.4	0.8	0.9	0.7
Brick compression				
number of tests	6	6	6	12
mean stress at failure (MPa)	8.89	17.95	19.49	11.58
standard deviation (MPa)	1.69	1.90	2.94	2.53
coefficient of variation	0.19	0.11	0.15	0.22
5th percentile stress at failure (MPa)	5.5	14.1	13.6	7.0

M *Minerva Crescent*
P *Pym Street*
S *South Road*
N *New bricks*

Direct tension

Mean direct tensile strength of the site-won bricks (see Table 6) varied from 1.60 to 1.98 MPa with coefficient of variation ranging between 0.25 and 0.37. The mean for the new bricks was 1.40 MPa, significantly lower than for the older units, with a coefficient of variation of 0.26. It was noted that the new bricks were a coarser texture, with coarser impurities which are likely to have contributed to the lower results for the new bricks.

Brick compression

The results for these tests which are also shown in Table 6 demonstrated mean compression strengths of the three site won specimens between 8.89 and 19.49 MPa, with coefficient of variation between 0.11 and 0.19. The mean for the new bricks was 11.58 MPa with a coefficient of variation of 0.22. Similar to the tests for direct tensile strength, the coarser texture and impurities are likely to have contributed to the lower results.

Relationship between tension and compression strengths

Compression strength data is often used to compare masonry materials and the ability to relate compression strength to tensile strength would allow useful comparisons for anchor capacities in various substrates. However, as can be seen from Fig. 21, there is minimal correlation between the compression and tension strengths which have been measured here (in Fig. 21,

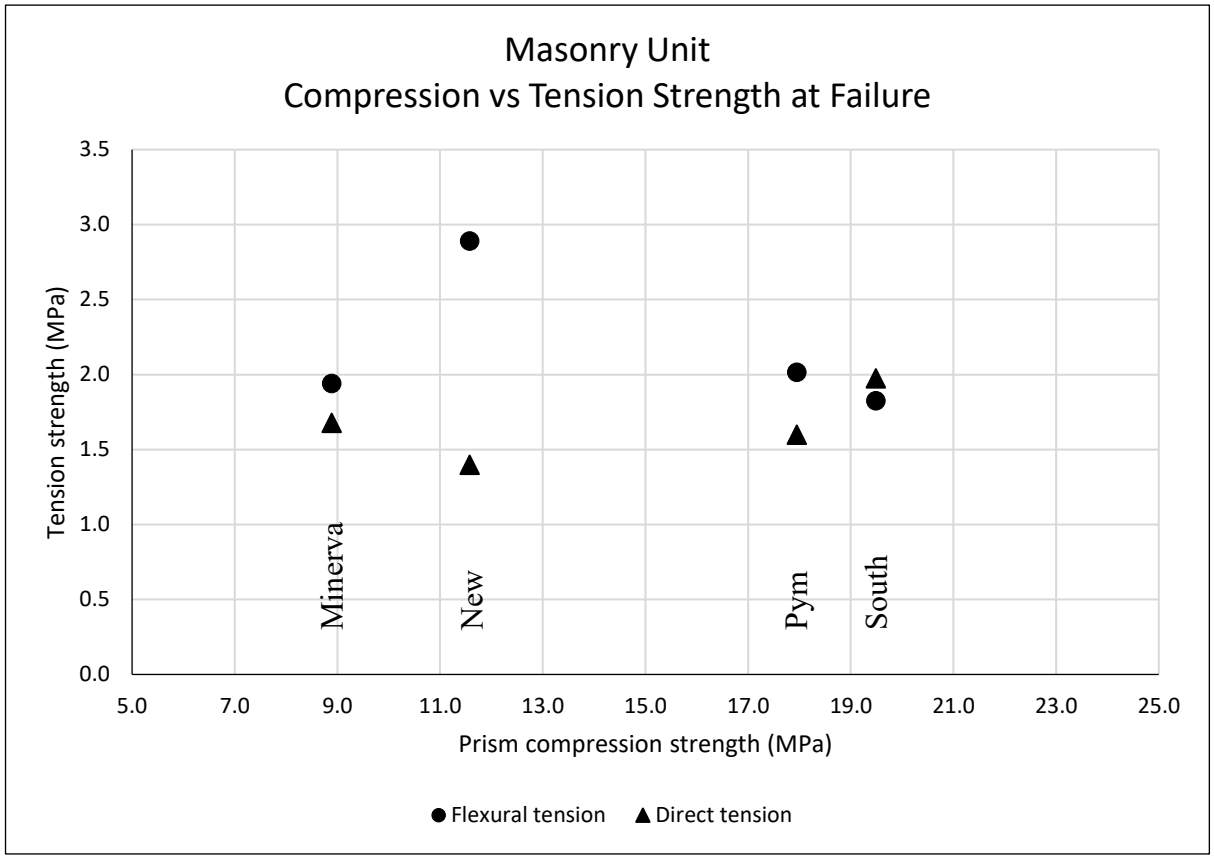

Fig. 21 – Material strength comparisons

Minerva, Pym and South refer to the sites where the older bricks were sourced, and New refers to new bricks). Further investigation of compression and direct tension strengths with larger sized test samples is recommended so that effects of texture and impurity coarseness is more comparable between tests, but not so large that masonry unit geometry (e.g. presence and size of frogs) impacts the results, rendering more useful output.

5.2. Anchor testing

For the quasi-static and cyclic anchor pull-out tests that have been undertaken in this research, the virtually exclusive failure mode has been splitting of the masonry unit with a subsequent extended softening region, as reported by Burton et al. (2020). The test configuration that has been adopted has excluded a cone/wedge failure for standard embedment depth tests, and clearly does not allow for brick pull-out failure, but even for poor installation tests, masonry splitting was still the exclusive failure mode. The exception to this were the poor quality installation tests that used short embedment where a cone failure was typical. The impact loading tests used masonry units that did not have lateral support and so the failure generally consisted of the brick splitting, without extended softening. Some typical anchor failures are shown in Figs. 22 to 25.

(a) Minerva Crescent

(b) Pym Street

(c) South Road

(d) New brick

Fig. 22 – Anchor failure under quasi-static loading with good installation

Fig. 23 – Anchor failure under cyclic loading – new brick

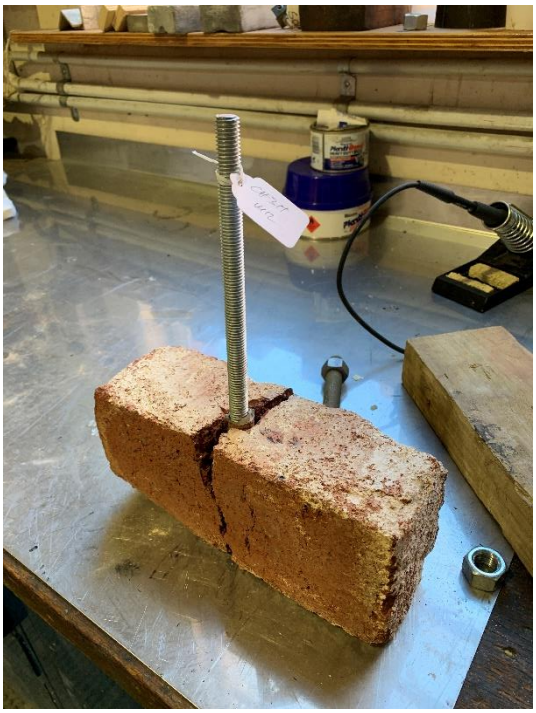

Fig. 24 – Anchor failure under impact loading – new brick

5.2.1. Quasi-static - good installation

The results for quasi-static tests with good installation are tabulated in Table 7. A feature of anchor failure associated with brick splitting where there is adequate cohesion between the bricks and mortar to provide lateral restraint is an extended softening region where the anchor capacity remains relatively constant over a large displacement. For the case of in-situ testing, this extended region is typified by the "In-situ" and the "Bending" result shown in Fig. 18.

Table 7 – Anchor pull out failure loads
(quasi-static – installed in accordance with manufacturers requirements)

Anchor peak pull out load (laboratory)					
	M	P	S(n)	S(w)	N
number of tests	12	12	12	9	12
mean failure load (kN)	10.78	12.86	8.57	11.78	13.30
standard deviation (kN)	1.69	3.52	3.12	2.57	1.89
coefficient of variation	0.16	0.27	0.36	0.22	0.14
5th percentile load at failure (kN)	7.7	6.5	3.0	7.0	9.9

M *Minerva Crescent*
P *Pym Street*
S(n) *South Road brick with no lateral confining resistance*
S(w) *South Road brick with 5kN lateral confining resistance*
N *New bricks*

These tests have been undertaken using 5 kN lateral confining resistance but there have also been a series of tests without the lateral resistance to ascertain the differences in peak pull-out load between the two scenarios and also to compare the values to those obtained by Burton

(a) short hole
(note localised cone failure)

(b) long hole

(c) not brushed

(d) not blown

Fig. 25 – Anchor failure under quasi-static loading with poor installation quality
(new bricks)

(e) not cleaned

(f) half filled

Fig. 25 (continued) – Anchor failure under quasi-static loading with poor installation quality (new bricks)

et al. (2020) from site which are shown in Table 8. Sorrentino et al. (2016), recommends modelling using the normal distribution for higher strength data (with coefficients of variation such that estimates of 5th percentile values are not negative). Based on this recommendation, the F-test has been applied and confirms that the variances of site to laboratory data for the site

Table 8 – Anchor pull out failure loads

Anchor peak pull out load (site)			
	M	P	S
number of tests	5	27	10
mean failure load (kN)	18.73	11.86	15.39
standard deviation (kN)	3.33	2.13	3.08
coefficient of variation	0.18	0.18	0.20
5th percentile load at failure (kN)	11.6	8.2	9.7

Data from Burton et al. (2020)
M *Minerva Crescent*
P *Pym Street*
S *South Road*

won bricks and site to laboratory data for new bricks are each from the same distribution at the 5% confidence level. Comparison of the mean values of the data sets (also at the 5% confidence level) shows that the results for the site-won bricks vary, with bricks from one of the sites (Pym) from the same distribution, but not so for the remaining two. This difference is likely to be explained by the presence of vertical confining stress in the in-situ tests but not in tests conducted in the laboratory and also, differences in actual cohesion, particularly in the case of

masonry units from one of the sites (Minerva) where the measured cohesion (Burton et al. 2020) was significantly greater than the 0.2MPa (Eq. 9) used here. The mean and 5th percentile peak pull-out capacities in all cases however are significantly greater than the tabulated characteristic capacity of 1.2 kN from the Hilti installation manual (Hilti 2019).

5.2.2. Quasi-static - poor installation

The results of 24 tests on new bricks conducted to determine what extent of load reduction can be expected as a consequence of poor installation practices are presented in Table 9. Observed

Table 9 – Poor quality installation – impact on peak pull out load

Anchor peak pull out load – poor quality installation (new bricks)								
Test type	Test label	Test Number	Peak pull out load (kN)	Count	Mean (kN)	Standard deviation (kN)	Coefficient of variation	5th percentile (kN)
Short hole	CH1BM12	1	7.17	4	7.60	0.42	0.06	6.60
	CH2BM12	2	7.30					
	CH13BM12	13	8.02					
	CH14BM12	14	7.90					
Long hole	CH3BM12	3	8.26	4	9.89	1.10	0.11	7.30
	CH4BM12	4	10.62					
	CH15BM12	15	10.20					
	CH16BM12	16	10.48					
Not brushed	CH5BM12	5	8.63	4	11.86	2.26	0.19	6.53
	CH6BM12	6	13.23					
	CH17BM12	17	13.61					
	CH18BM12	18	11.96					
Not blown	CH7BM12	7	9.51	4	9.68	0.66	0.07	8.11
	CH8BM12	8	8.98					
	CH19BM12	19	9.65					
	CH20BM12	20	10.57					
Not cleaned	CH9BM12	9	8.99	4	9.17	0.33	0.04	8.39
	CH10BM12	10	8.97					
	CH21BM12	21	9.66					
	CH22BM12	22	9.06					
Half filled	CH11BM12	11	11.84	4	11.74	2.29	0.19	6.37
	CH12BM12	12	8.88					
	CH23BM12	13	14.48					
	CH24BM12	24	11.77					

C ⇒ *Chemical anchor*
H ⇒ *Hilti HIT-HY 170 injection mortar*
B ⇒ *Bad (poor quality installation – new bricks*
M12 ⇒ *M12 threaded rod anchors*

underperformance of chemical anchors is often attributed to poor site practices but these results suggest that this is not the case. The Hilti installation manual (Hilti 2019) recommends a characteristic capacity of 1.2 kN for the type of anchor, adhesive and brick that has been used in these tests which is considerably lower than any of the measured means and 5th percentile

values as shown in Fig. 26. This suggests that even with these poor installation practices, the underperformance noted by Dizhur et al. (2016) should not be attributed to these issues.

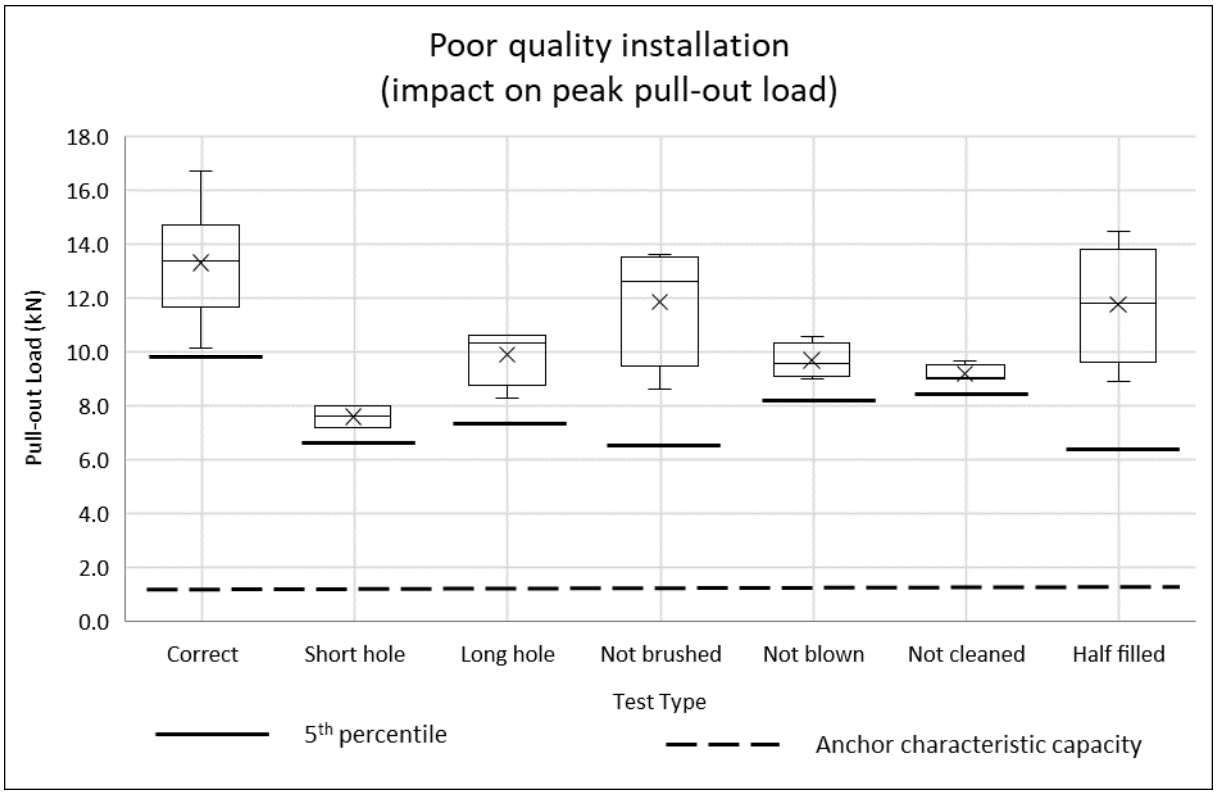

Fig. 26 – Poor quality installation
(impact on peak pull-out load)

5.2.3. Impact testing

The results of these tests are shown in Table 10 and the adjusted pull-out loads taking account of the dynamic load associated with the anchor and measuring equipment are shown in Fig. 27. As can be seen from the figure, the adjusted mean is only slightly lower than the quasi-static mean and consequently, it can be concluded that dynamic loads do not influence the anchor strength significantly. There is however greater variability in the data resulting in a 5th percentile pull-out load of 4.6 kN, compared to 9.9 kN for the same bricks under quasi-static loading. Therefore further study with a greater number of samples and acceleration rates more closely aligned to real world (earthquake, wind) loading is warranted. However, the 5th percentile value is still considerably larger than the Hilti characteristic capacity (Hilti 2019) and it is therefore unlikely that high rate loading contributes to the observed underperformance (Dizhur et al. 2016).

Table 10 – Impact test data

Anchor peak pull out load			
	Brick	Styrene	Adjusted
number of tests	12	3	12
mean failure load (kN)	19.85	8.32	11.53
standard deviation (kN)	3.83	0.85	3.83
coefficient of variation	0.19	0.10	0.33
5th percentile load at failure (kN)	12.97	5.84	4.64

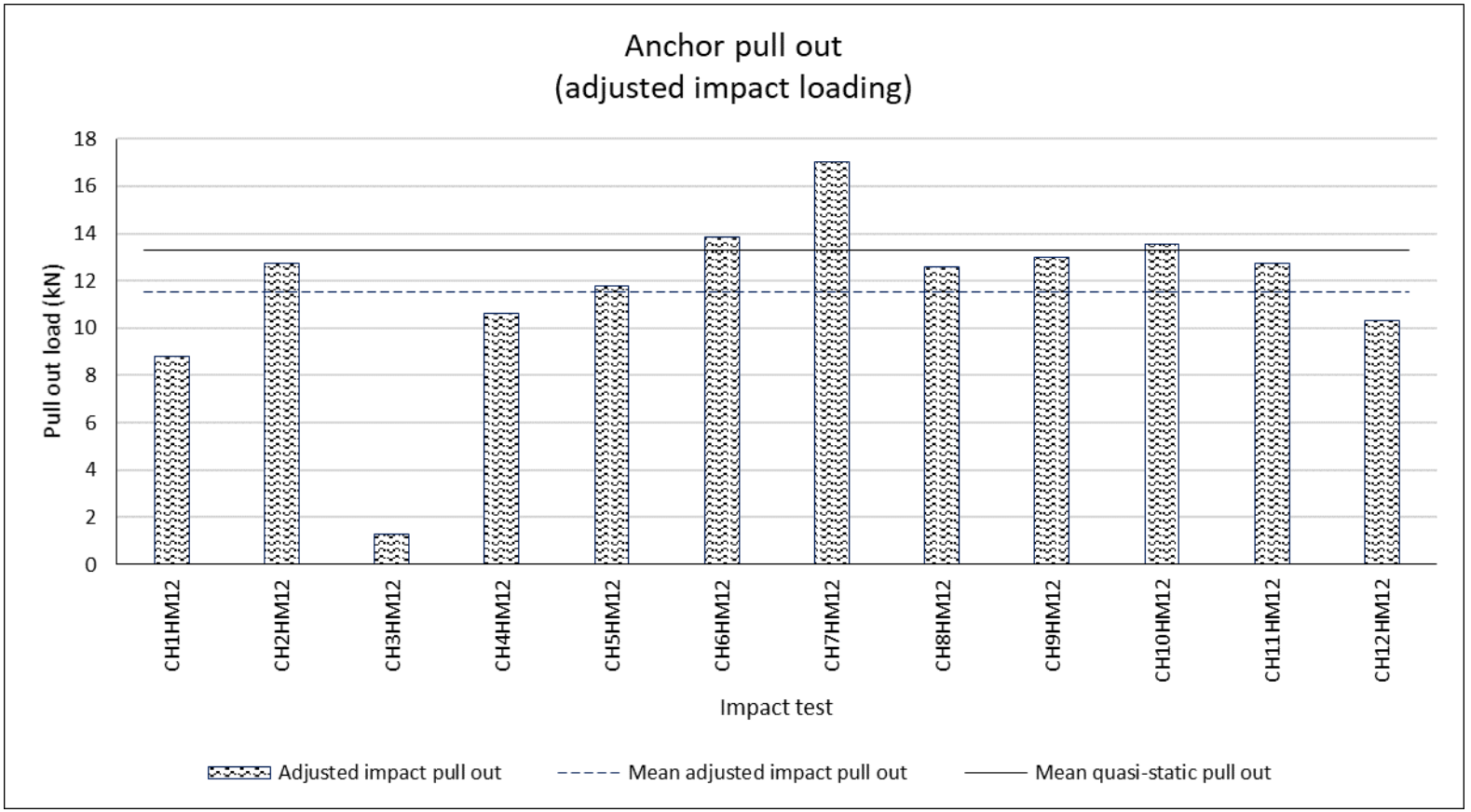

Fig. 27 – Adjusted impact loading

5.2.4. Cyclic testing

One each of load-controlled and displacement-controlled tests on new bricks were undertaken as it was expected that due to the observed extended softening region that the cyclic loading would have minimal impact over time on the load capacity but exhibit ongoing hysteresis with each cycle. This expectation was realised (refer Fig. 28) with the implication that cyclic loading does not significantly impact the overall load capacity of the anchor and the load capacity remains well above the characteristic resistance although as can be seen in this figure, (particularly for the displacement-controlled case), there is some cycle-to-cycle degradation.

6. Summary, conclusions and recommendations

Underperformance of masonry anchors has been implicated in failure of strengthened unreinforced masonry in the 2011 Christchurch earthquake. Recent site investigations of vintage masonry structures has identified that failure of chemical anchors installed in masonry is through a splitting mechanism whereby the influence of wedging and bending stresses from anchor loading within the units results in the brick splitting. This allows the anchor to be extracted under a lesser load than the more commonly considered cone type of failure, or of the entire masonry unit being extracted from the wall. A detailed laboratory experimental campaign has been undertaken to investigate the splitting failure mechanism which has confirmed that this can be a dominant failure mode in masonry when chemical anchors are loaded in tension.

Many investigators have previously observed splitting of masonry units under anchor pull-out loading but have attributed this to being an artefact of the adhesive bond failure between the anchor rod and the substrate rather than being a critical failure mode. An important consequence of the splitting failure is that following initial failure of the masonry unit (in splitting), whilst there is a reduction in anchor capacity, the reduction remains relatively constant and considerable anchor strength remains. This is because lateral restraint of the brick from the physical mass of the wall, through cohesion between masonry units, provides resistance to the wedging forces as the anchor is further extracted. If the anchors are deeply embedded in the masonry, then as a consequence of non-uniform stress distribution along the anchor, it is likely that splitting of face units will occur before the peak load has been reached, obfuscating the importance of the brick splitting. Furthermore, the test configuration can also obscure the early occurrence of splitting by physically hiding the test location with the testing apparatus, or by developing excessive global horizontal bending moments which reduce the internal bending stresses within the brick.

Recognising that splitting failure from wedging and bending stresses within the brick is critical to understanding the failure mechanism of masonry anchors, a new laboratory test approach has been developed which is able to simulate the internal bending moments within the brick and also apply the necessary lateral loads to provide the required restraint to the wedging forces. Of particular importance is that this new test is able to be conducted on single masonry units making it a simple and inexpensive test allowing a much greater number of tests to be performed when compared to more common approaches requiring sample “walls” to be constructed.

As a direct result of this simplified testing methodology, a large number of tests have been conducted which have covered good and poor-quality installation, and the effects on pull-out-capacity resulting from cyclic and impact loading on chemical anchors. These tests have

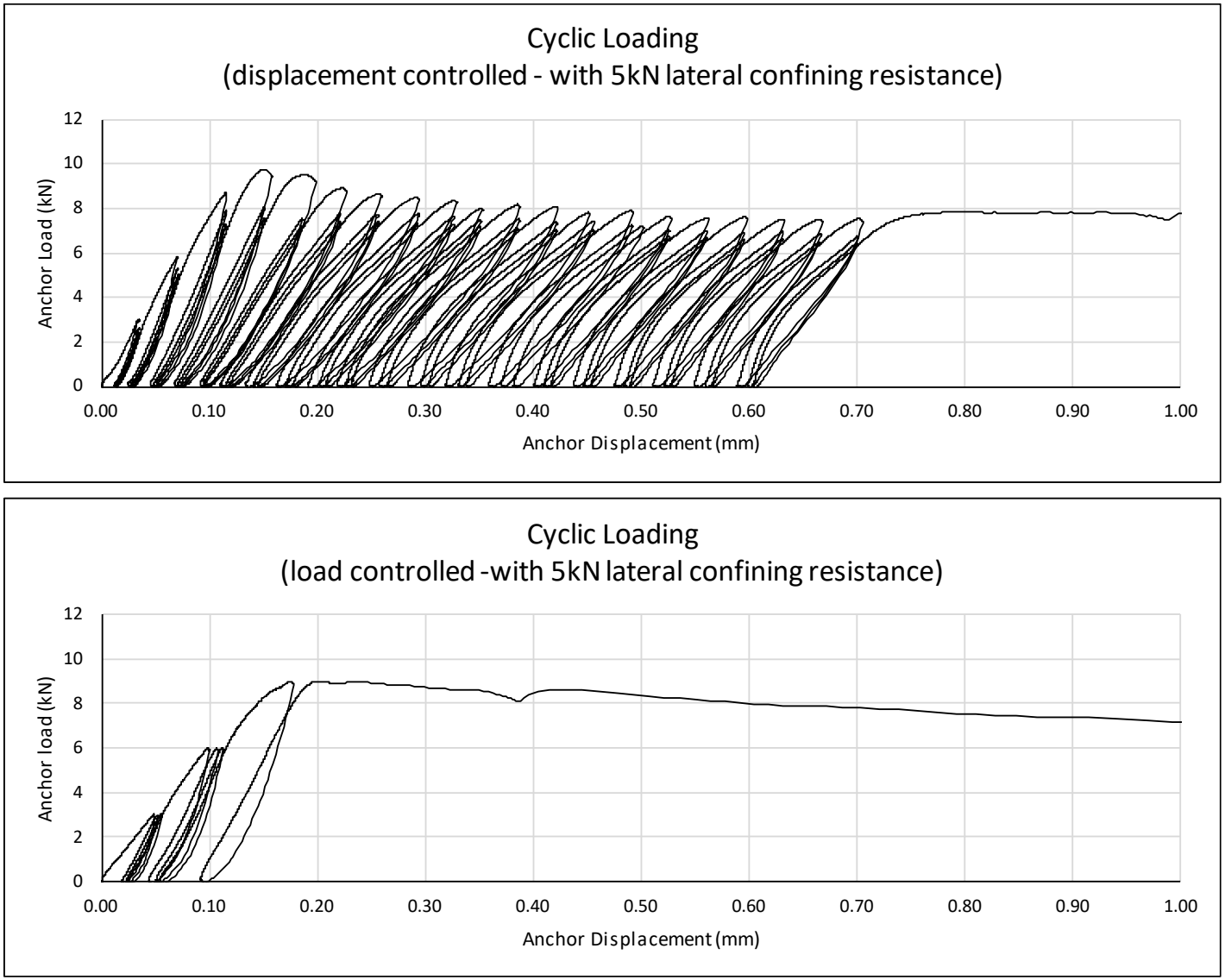

Fig. 28 – Cyclic loading

demonstrated that provided adequate cohesion between masonry units remains, the lateral restraining forces which develop in the masonry which resist the wedging stresses continue after the brick has split. In particular with regards to the splitting failure, this results in an extended softening where the anchor pull-out-capacity remains greater than the anchor characteristic capacity which limits the strength reduction which may otherwise result from cyclic loading. Tests of anchors subjected to high-rate impact loading also suggest that there is only a small reduction in anchor strength as a result of impact loading and tests which looked at various poor installation scenarios also suggest that installation quality has only a small effect on anchor strength. It is therefore suggested that cyclic and impact loading as well as poor quality installation of anchors does not significantly reduce the pull-out strength of chemical anchors and consequently, they have minimal impact on earthquake strengthening.

The investigations undertaken here covering quasi-static, cyclic and impact loading, indicate that based on traditional design approaches for chemical anchors, that even with peak ground accelerations considerably greater than design values as occurred in Christchurch in 2011, that there exist adequate factors of safety such that anchor underperformance should not have been a causative factor in structural failures. However, splitting failure of masonry units can lead to reduced anchor strength and may explain the observed underperformance, particularly if loss of cohesion reduces lateral restraint. Further research looking at the time history of anchor loading (including oscillatory motion from seismic events) and loss of lateral restraint, particularly focusing on early life masonry unit splitting, and development of a design model for this type of failure that can be applied to the full design life of chemical anchors is required.

Appendix A

Load distribution from wall to restraint system

Let us consider the stresses that develop in a single masonry unit with an anchor located centrally when the wall is excited in the out-of-plane direction and restrained by being anchored to some supplementary structure with typical arrangement as depicted in Fig. A1 which uses the following nomenclature:

l_1 *length of a brick plus one mortar joint*
l_2 *horizontal anchor spacing*
h_1 *height of a brick plus one mortar joint*
h_2 *unsupported wall height above the line of anchors*
h_3 *vertical distance between diaphragm and support line*
h_4 *out-of-plane load contribution below the support line*
h_5 *vertical distance between diaphragms or diaphragm and wall footing*
h_6 *vertical extent of the horizontal load contribution based on two way bending*

Out-of-plane load
Assuming that the out-of-plane load is generated by wind or seismic action, the total out of plane load P_{tot} that is applied to each anchor is a function of the contributory wall area and therefore,

$$P_{tot} = k_1 l_2 (h_2 + h_4) \qquad (A1)$$

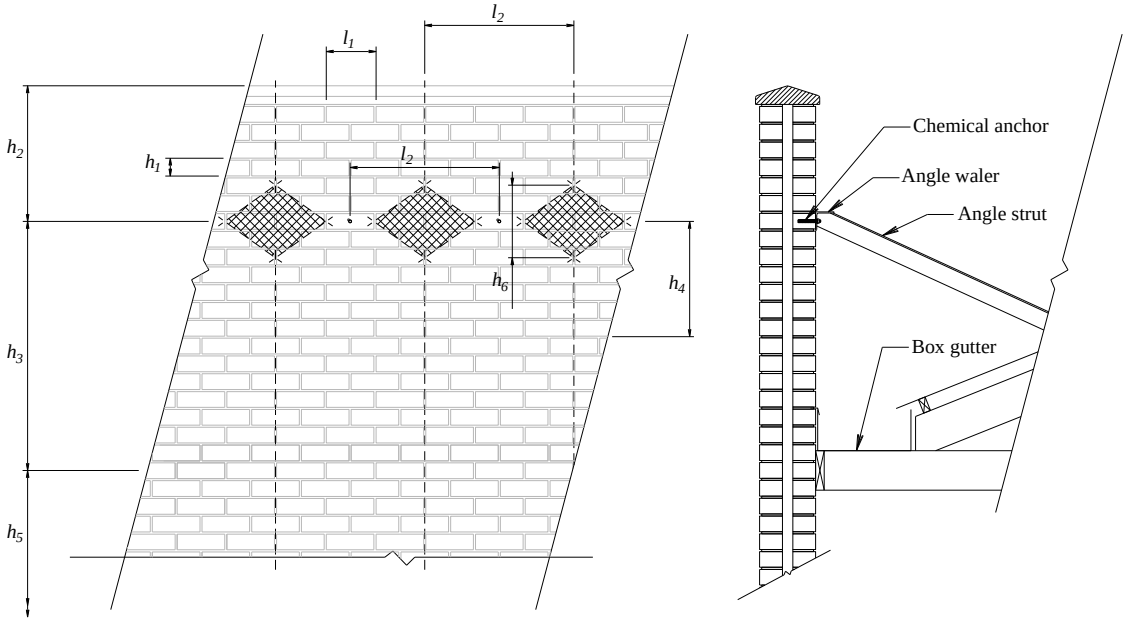

(a) Tributary areas (b) Typical arrangement

Fig. A1 – Wall to support structure load transfer

where k_1 is the ratio of wall area to load. The component of that load generated from horizontal bending, assuming regular two way bending in the masonry, P_{hor} is depicted by the shaded areas in Fig. A1 and is given by:

$$P_{hor} = k_1 l_2 h_6 \tag{A2}$$

and as h_6 is a function of the brick and mortar dimensions, then:

$$P_{hor} = k_1 l_2 \left(\frac{l_2 h_1}{l_1}\right) \tag{A3}$$

and as the component of the load from vertical bending (P_{vert}) is simply the compliment of the total load and the horizontal component, then:

$$P_{vert} = k_1 l_2 \left[(h_2 + h_4) - \left(\frac{l_2 h_1}{l_1}\right)\right] \tag{A4}$$

Load transfer to brick

The component of the load from vertical bending transfers to the anchored masonry unit as out-of-plane shear through cohesion and friction between the above and below mortar joints (assuming that the perpends are incompletely filled and contribute minimally). This load can

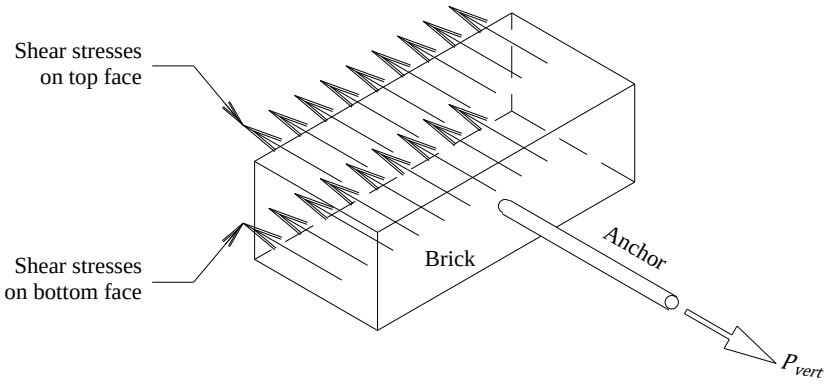

(a) Pictorial representation

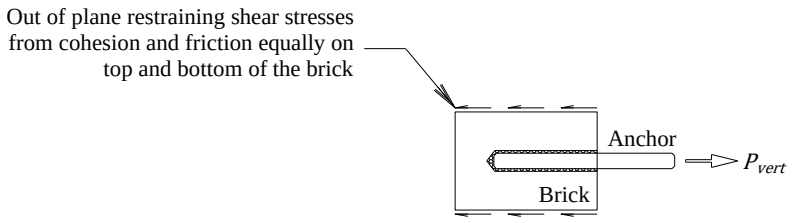

(b) Section at anchor

Fig. A2 – Vertical load contribution to anchored brick

be considered as a uniformly distributed load (UDL) on the top and bottom faces of the anchored brick as shown in Fig. A2.

The component of the load from horizontal bending transfers to the anchored brick as an out-of-plane shear uniformly distributed over the top and bottom faces of the brick through load transfer via the courses above and below, and also, as a horizontal bending moment is induced in the wall, there is a torsion component, centred on the quarter points of the loaded brick, again transferred through the courses above and below, on the top and bottom faces, as shown in Fig. A3.

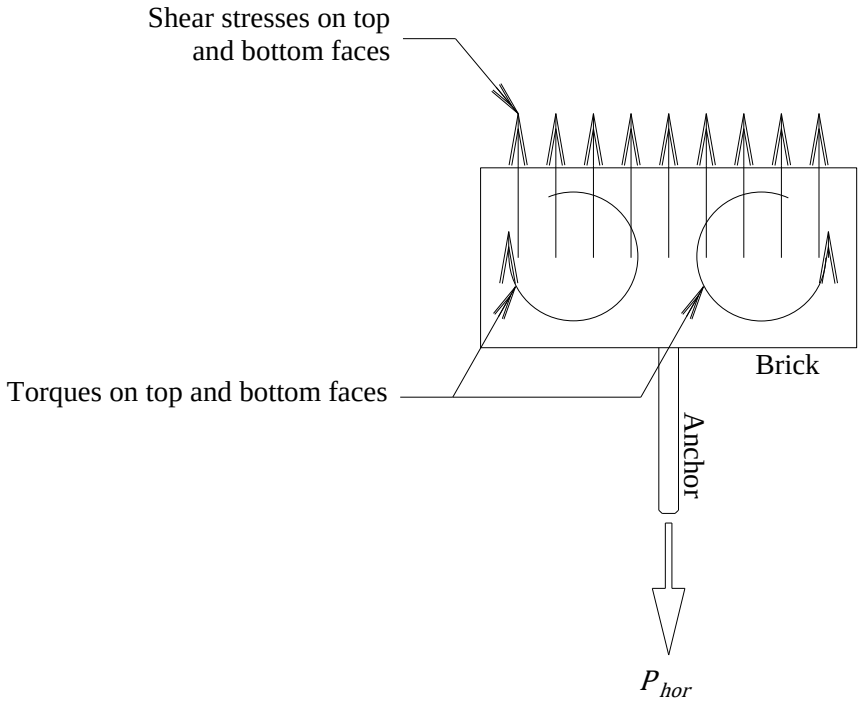

Fig. A3 – Horizontal load contribution to anchored brick

The total out-of-plane shear transferred to the brick from the horizontal and vertical contributions is equal to P_{tot} as given by Eq. (A1), but the torsion associated with the global bending moment is an additional contribution to be considered. Based on the notional configuration shown in Fig. A1, the bending moment at the quarter points of the anchored bricks is slightly less than 60% of the peak (negative) bending moment which is proportional to the peak component of that load generated from horizontal bending P_{hor}.

The contribution of horizontal compared to the total shear load on the brick is given by:

$$\frac{P_{hor}}{P_{tot}} = \frac{k_1 l_2 \left(\frac{l_2 h_1}{l_1}\right)}{k_1 l_2 (h_2 + h_4)} \tag{A5}$$

$$= \frac{\left(\frac{l_2 h_1}{l_1}\right)}{(h_2 + h_4)} \tag{A6}$$

In the typical masonry strengthening as shown in Fig. A1, the contributory load height ($h_2 + h_4$) is in the order of 15 times the masonry unit height plus mortar joint and using this, Eq. (A6) can be expressed as:

$$\frac{P_{hor}}{P_{tot}} = \frac{\left(\frac{l_2 h_1}{l_1}\right)}{15h_1} = \frac{l_2}{15l_1} \qquad (A7)$$

In the configuration presented in Fig. A1, $l_2/l_1 = 3$, meaning that P_{hor} is 20% of P_{tot} which results in the torsion applied to the masonry unit being a negative 33% of the total bending in the brick as a result of the applied UDL assuming that the brick has not split. If the brick is already split, then this torsion adds to the bending moment.

Appendix B

Load / slip relationship for chemical anchors in masonry units under differing lateral confining loads with typical load / slip behaviour from in-situ testing

Fig. B1 provides the basis of the experimental test designation used throughout the paper and Figs. B2-B6 provide the experimental load slip relationships for 0, 2,5,10 and 15 kN lateral confining resistance respectively

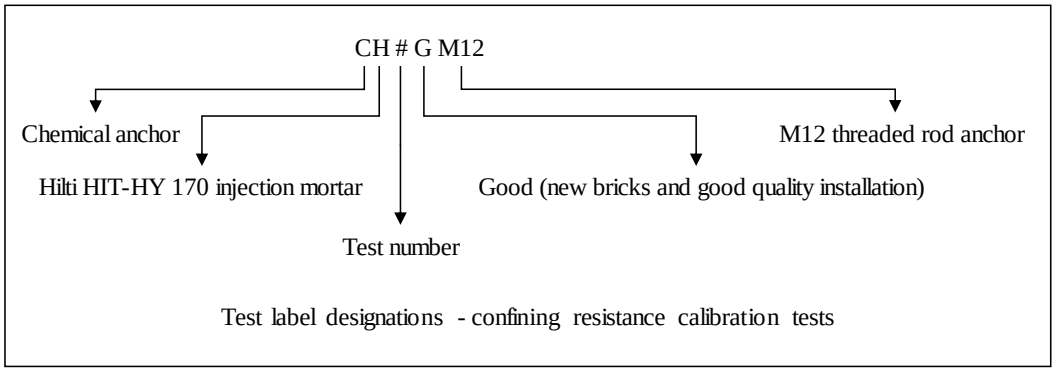

Fig. B1 Experimental test designations

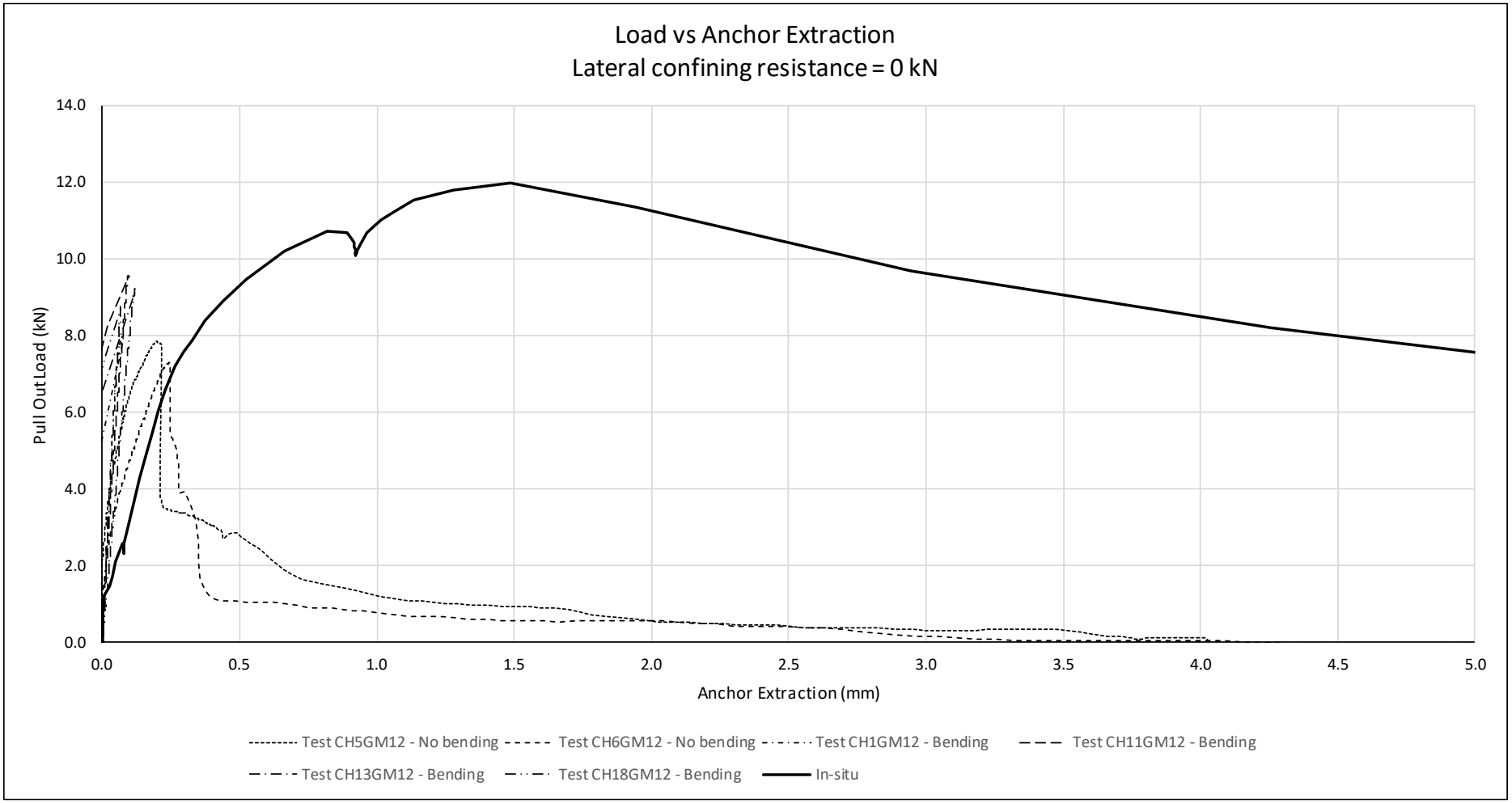

Fig. B2 – Load/slip relationship for anchor extraction with 0 kN lateral confining resistance

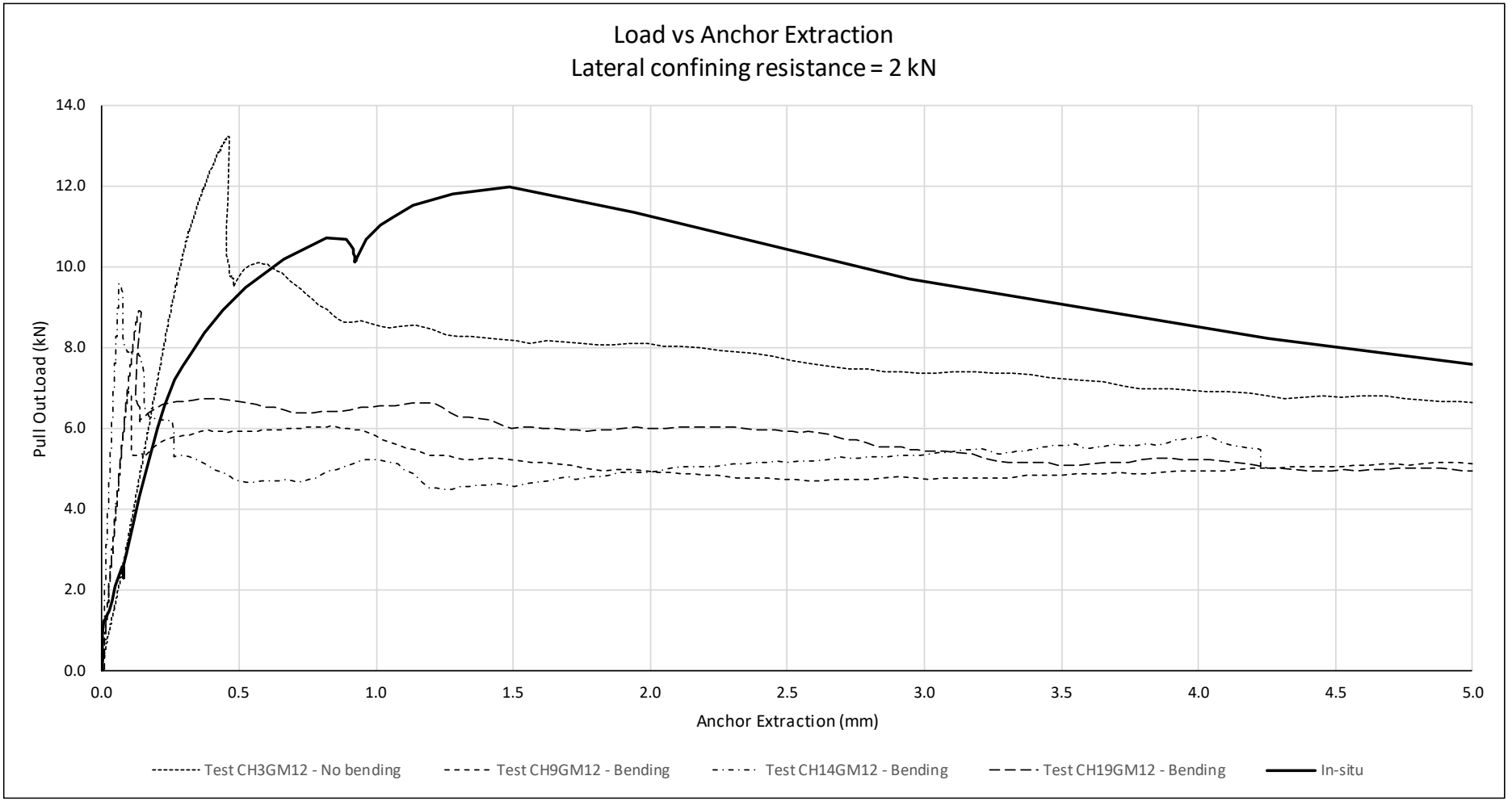

Fig. B3 – Load/slip relationship for anchor extraction with 2 kN lateral confining resistance

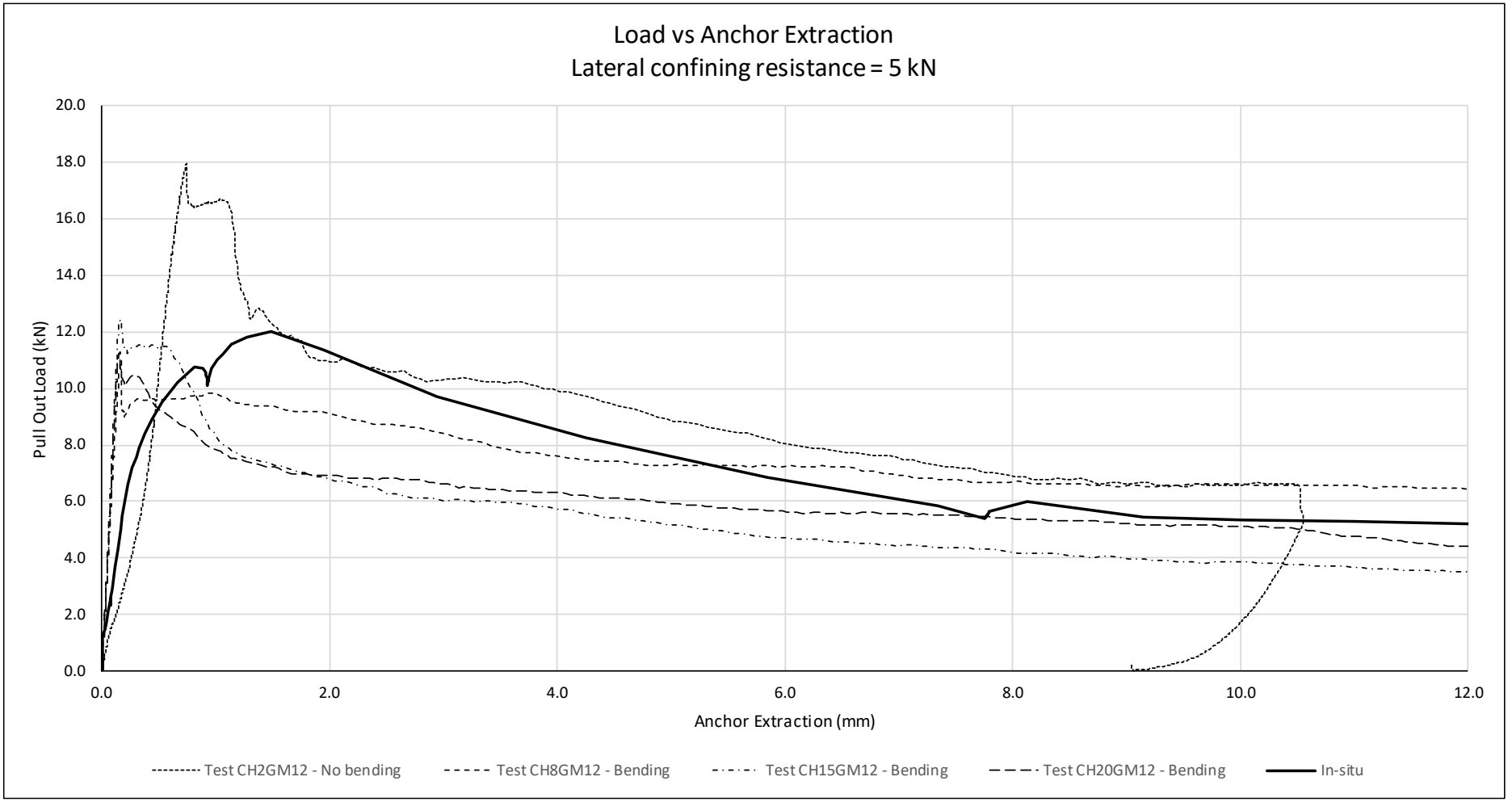

Fig. B4 – Load/slip relationship for anchor extraction with 5 kN lateral confining resistance

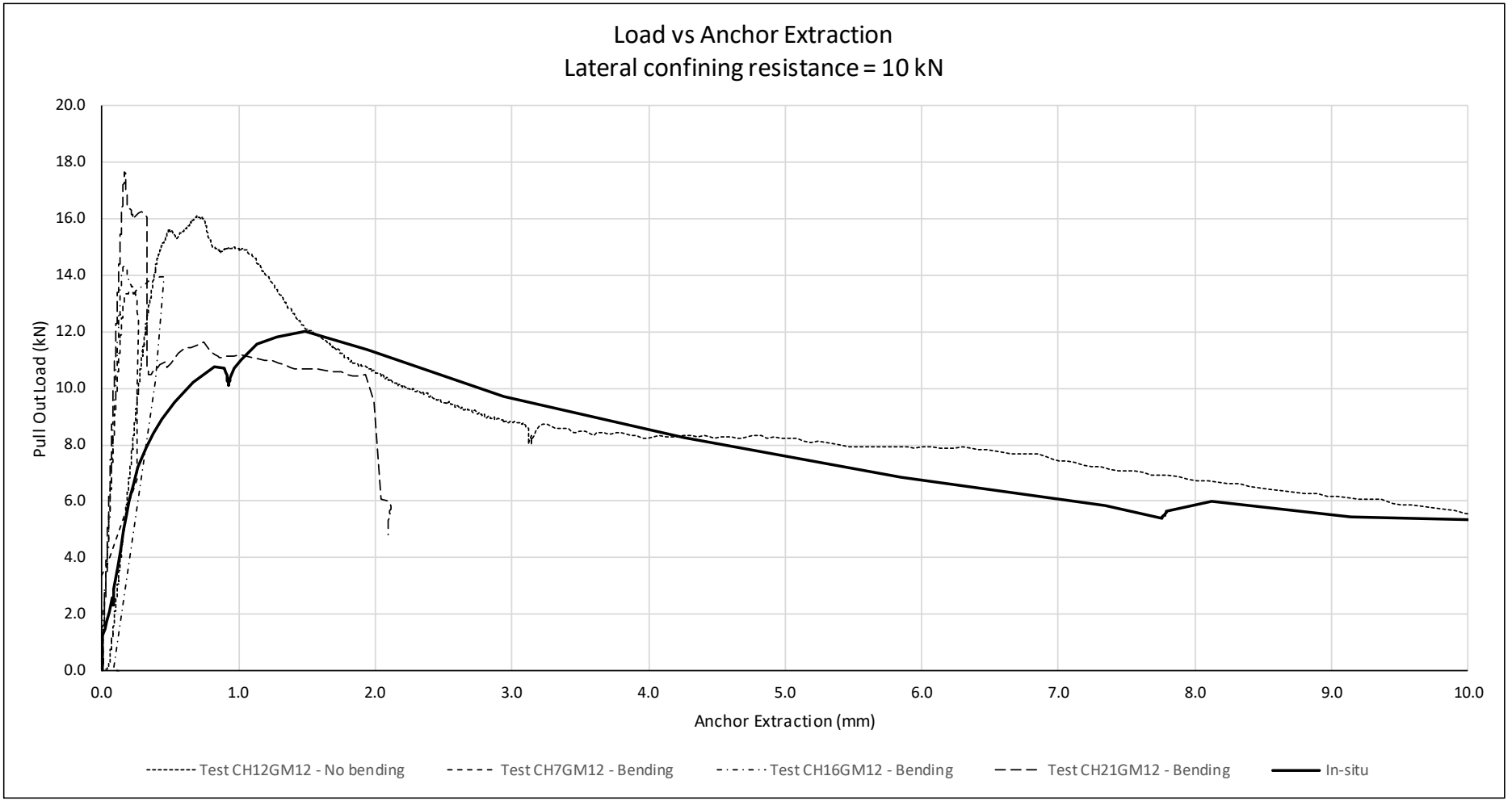

Fig. B5 – Load/slip relationship for anchor extraction with 10 kN lateral confining resistance

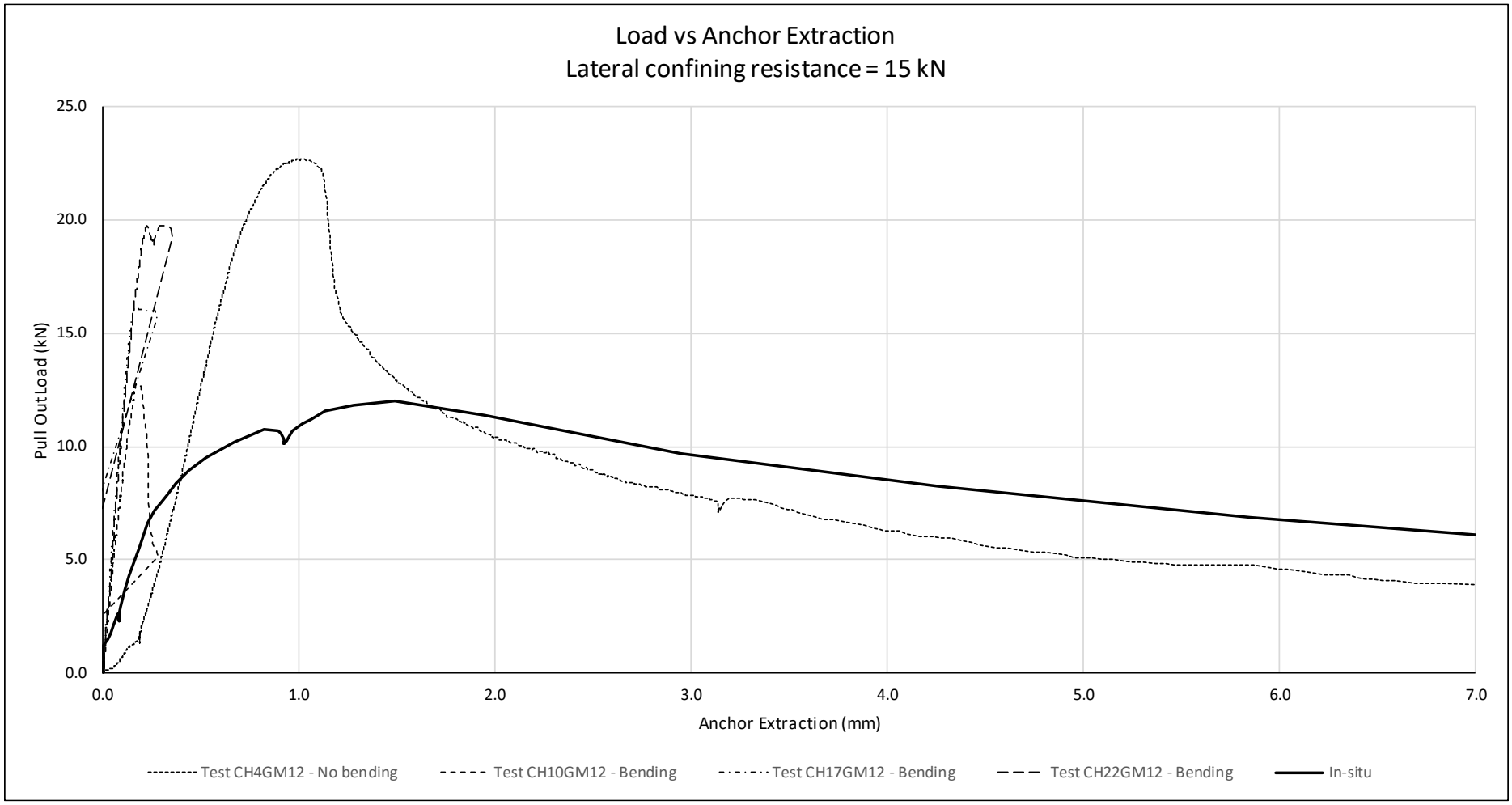

Fig. B6 – Load/slip relationship for anchor extraction with 15 kN lateral confining resistance

Acknowledgements
This project was supported by funds awarded under the Australian Research Council Discovery Project No. DP190100797. However, the views expressed in this paper are those of the authors and not necessarily those of the sponsor. The authors also wish to thank Mr Ian Ogier from the University of Adelaide Civil Engineering Structures Laboratory for his assistance with some of the testing.

References

Arifovic, F. and M. P. Nielsen (2006). Strength of anchors in masonry.

Burton, C., P. Visintin, M. Griffith and J. Vaculik (2020). "Field testing of vintage masonry: Mechanical properties and anchorage strengths." Structures **28**: 1900-1914.

Ceroni, F., M. Di Ludovico and A. Balsamo (2020). "Effectiveness of design formulations for injected anchors in masonry elements." Journal of Building Pathology and Rehabilitation **5**(1): 1-12.

Dizhur, D., A. Schultz and J. Ingham (2016). "Pull-Out Behavior of Adhesive Connections in Unreinforced Masonry Walls." Earthquake Spectra **32**(4): 2357-2375.

Eligehausen, R., R. Cook and J. Appl (2006). "Behavior and design of adhesive bonded anchors." ACI Structural Journal **103**: 822-831.

Fuchs, W. (2001). Evolution of fastening design methods in Europe. Connections between steel and concrete, Stuttgart, Germany, University of Stuttgart.

Giresini, L., M. L. Puppio and F. Taddei (2020). "Experimental pull-out tests and design indications for strength anchors installed in masonry walls." Materials and Structures **53**(4): 1-16.

Hatzinikolas, M. A., R. Lee, J. Longworth and J. Warwaruk (1983). "Drilled-in inserts in masonry construction."

Hilti (2019). Hilti Anchor Fastening Technology manual.

Lee, J. and E. Gad (2017). Design guidelines for post-installed and cast-in anchors in Australia for safety-critical applications. Austroads Bridge Conference, 10th, 2017, Melbourne, Victoria, Australia.

McGinley, W. (2006). "Design of anchor bolts in masonry." Progress in Structural Engineering and Materials - PROG STRUCT ENG MATER **8**: 155-164.

Megget, L. M. (2006). "From brittle to ductile." Bulletin of the New Zealand Society for Earthquake Engineering **39**(3): 158-169.

Miccoli, L., P. Fontana, S. Paganoni and D. D'Ayala (2015). "Pull-out strength of anchor pins for brickwork masonry and earth block masonry / Auszugsfestigkeit von Verpressankern für Ziegel- und Lehmsteinmauerwerk." Mauerwerk **19**(5): 383-393.

Moon, L., D. Dizhur, I. Senaldi, H. Derakhshan, M. Griffith, G. Magenes and J. Ingham (2014). "The Demise of the URM Building Stock in Christchurch during the 2010–2011 Canterbury Earthquake Sequence." Earthquake Spectra **30**(1): 253-276.

Muñoz, R. and P. B. Lourenço (2019). Mechanical Behaviour of Metal Anchors in Historic Brick Masonry: An Experimental Approach. Structural Analysis of Historical Constructions, Springer**:** 788-798.

Munoz, R., P. B. Lourenco and S. Moreira (2018). "Experimental results on mechanical behaviour of metal anchors in historic stone masonry." Construction and Building Materials **163**: 643-655.

Nielsen, M. P. and L. C. Hoang (2016). Limit analysis and concrete plasticity, third edition, CRC Press.

Page, A. W. (2002). "Unreinforced masonry structures – An Australian overview."

Pisani, M. A. (2016). "Theoretical approach to the evaluation of the load-carrying capacity of the tie rod anchor system in a masonry wall." Engineering Structures **124**: 85-95.

Powers (2017). "ANCHORING & FASTENING SYSTEMS Technical Manual for the Design Professional."

Ramset (2019). "Specifiers Anchoring Resource Book ANZ Edition 2."

Sorrentino, L., P. Infantino and D. Liberatore (2016). Statistical tests for the goodness of fit of mortar compressive strength distributions: Proceedings of the 16th International Brick and Block Masonry Conference, Padova, Italy, 26-30 June 2016.

Standards Australia (2003). AS/NZS 4456.15:2003 - Masonry units, segmental pavers and flags—Methods of test. Method 15: Determining lateral modulus of rupture.

Standards Australia (2018). AS 3700 - Masonry structures.

Vaculik, J. and M. C. Griffith (2017). "Probabilistic analysis of unreinforced brick masonry walls subjected to horizontal bending." Journal of Engineering Mechanics **143**(8): 04017056.